

Wind forcing impact over water dynamics and shelf - deep sea exchange processes

Andrei Zatsepin and V.V. Kremenetskiy

P.P. Shirshov Institute of Oceanology, Moscow, Russia
zatsepin@ocean.ru

with contributions from: A. Arashkevich, A. Kostianoy and V. Zhurbas

International Conference (school-seminar) “Dynamics of Coastal Zone of Non-tidal Seas” (Baltiyisk, 30 June – 05 July, 2008)

Content of the presentation

- some theoretical aspects of wind-driven circulation in coastal zone and open sea;
- wind forcing impact on Black Sea dynamics and shelf-deep sea interaction (field observations, laboratory and numerical modeling);
- influence of Black Sea dynamics on zooplankton distribution between coastal zone and open sea.

Wind stress: definition and bulk formula

The horizontal force of the wind on the sea surface is called the **wind stress**

$$\tau = \rho_a \cdot C_d \cdot U_a^2$$

$$\tau = \{\tau_x, \tau_y\}$$

$\rho_a \approx 1.3 \cdot 10^{-3} \text{ g/cm}^3$ – air density; $C_d \approx (1-2) \cdot 10^{-3}$ – drag coefficient; U_a – wind speed at 10 m

U_a , m/s	τ , dyn/cm ²
2	0.05
7	1.0
20	10

Basic equations

$$\frac{du}{dt} = -\frac{1}{\rho} \frac{\partial p}{\partial x} + fv + \frac{\partial}{\partial z} (A_z \frac{\partial u}{\partial z})$$

boundary conditions

$$\tau_x = \rho A_z \frac{\partial u}{\partial z} \Big|_{z=0}$$

$$\frac{dv}{dt} = -\frac{1}{\rho} \frac{\partial p}{\partial y} - fu + \frac{\partial}{\partial z} (A_z \frac{\partial v}{\partial z})$$

$$\tau_y = \rho A_z \frac{\partial v}{\partial z} \Big|_{z=0}$$

$$\frac{dw}{dt} = -\frac{1}{\rho} \frac{\partial p}{\partial z} - g$$

$$\frac{\partial u}{\partial x} + \frac{\partial v}{\partial y} + \frac{\partial w}{\partial z} = 0$$

Ekman's solution (Ekman, 1905)

$$\frac{\partial}{\partial t} = \frac{\partial}{\partial x} = \frac{\partial}{\partial y} = 0; \rho, A_z = \text{const}; H \rightarrow \infty$$

$$fv + A_z \frac{\partial^2 u}{\partial z^2} = 0 \quad u = V_0 \exp^{-az} \cos(\pi/4 + az)$$

$$fv + A_z \frac{\partial^2 v}{\partial z^2} = 0 \quad v = V_0 \exp^{-az} \sin(\pi/4 + az)$$

$$a = \sqrt{\frac{f}{2A_z}} \quad V_0 = \sqrt{\frac{\tau}{\rho^2 f A_z}} \quad H_E = \sqrt{\frac{2\pi^2 A_z}{f}}$$

Example:

$$\tau = 1 \text{ dyn/cm}^2, f = 10^{-4} \text{ c}^{-1}, A_z = 10 \text{ cm}^2/\text{s} \quad \longrightarrow \quad V_0 = 30 \text{ cm/s}, H_E = 13 \text{ m}$$

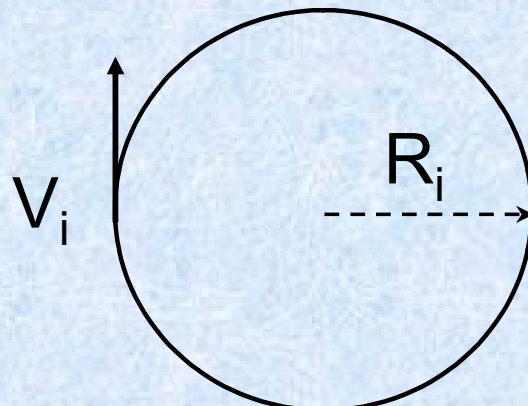
Inertial oscillations

$$\frac{\partial}{\partial x} = \frac{\partial}{\partial y} = 0; \quad \tau, A_z = 0; \quad \rho = \text{const}; \quad H \rightarrow \infty$$

$$\frac{du}{dt} = fv \quad u = V_i \sin(ft)$$

$$\frac{dv}{dt} = -fu \quad v = V_i \cos(ft)$$

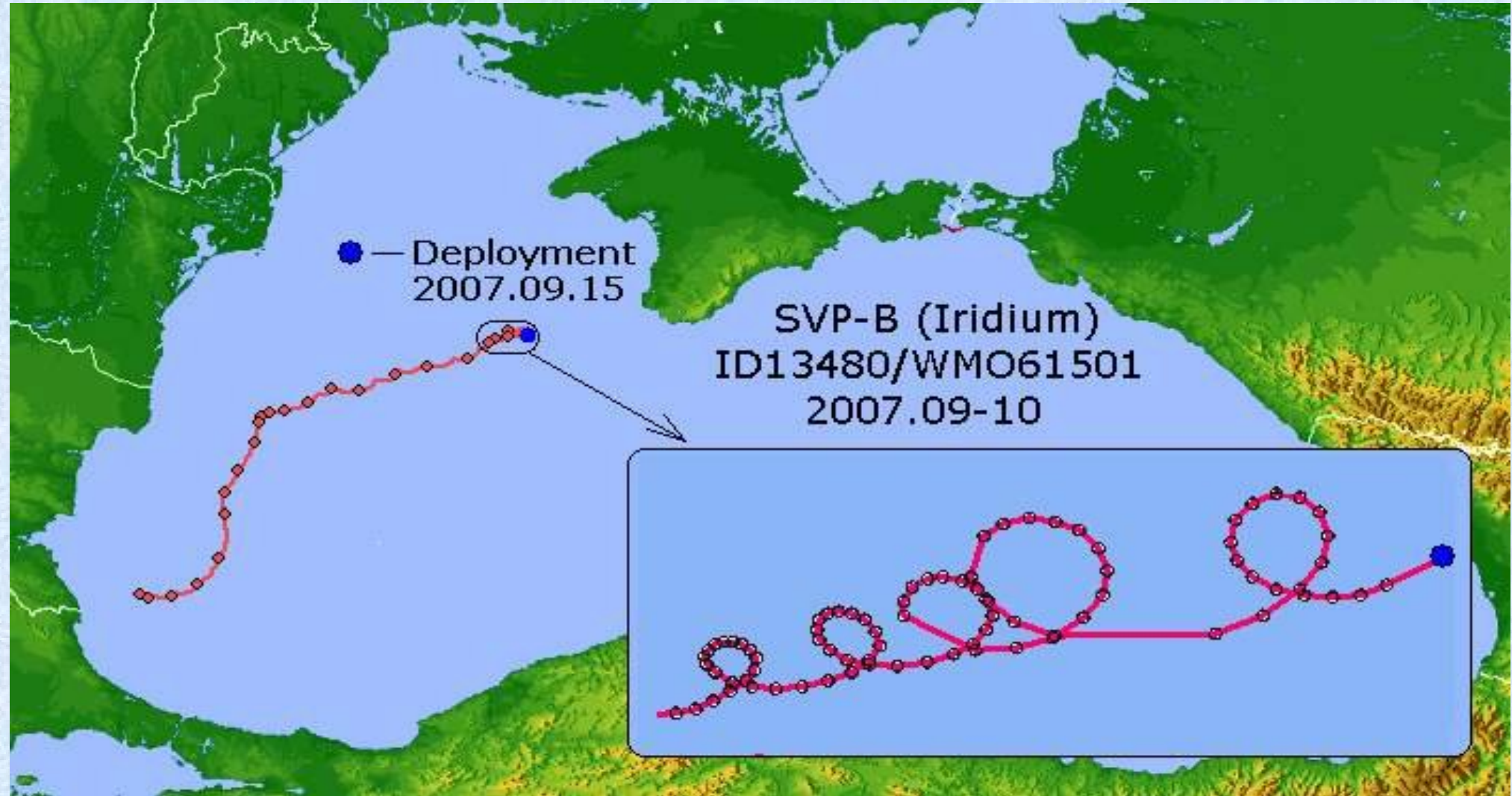
$$V_i^2 = u^2 + v^2 \quad R_i = \frac{V_i}{f}$$



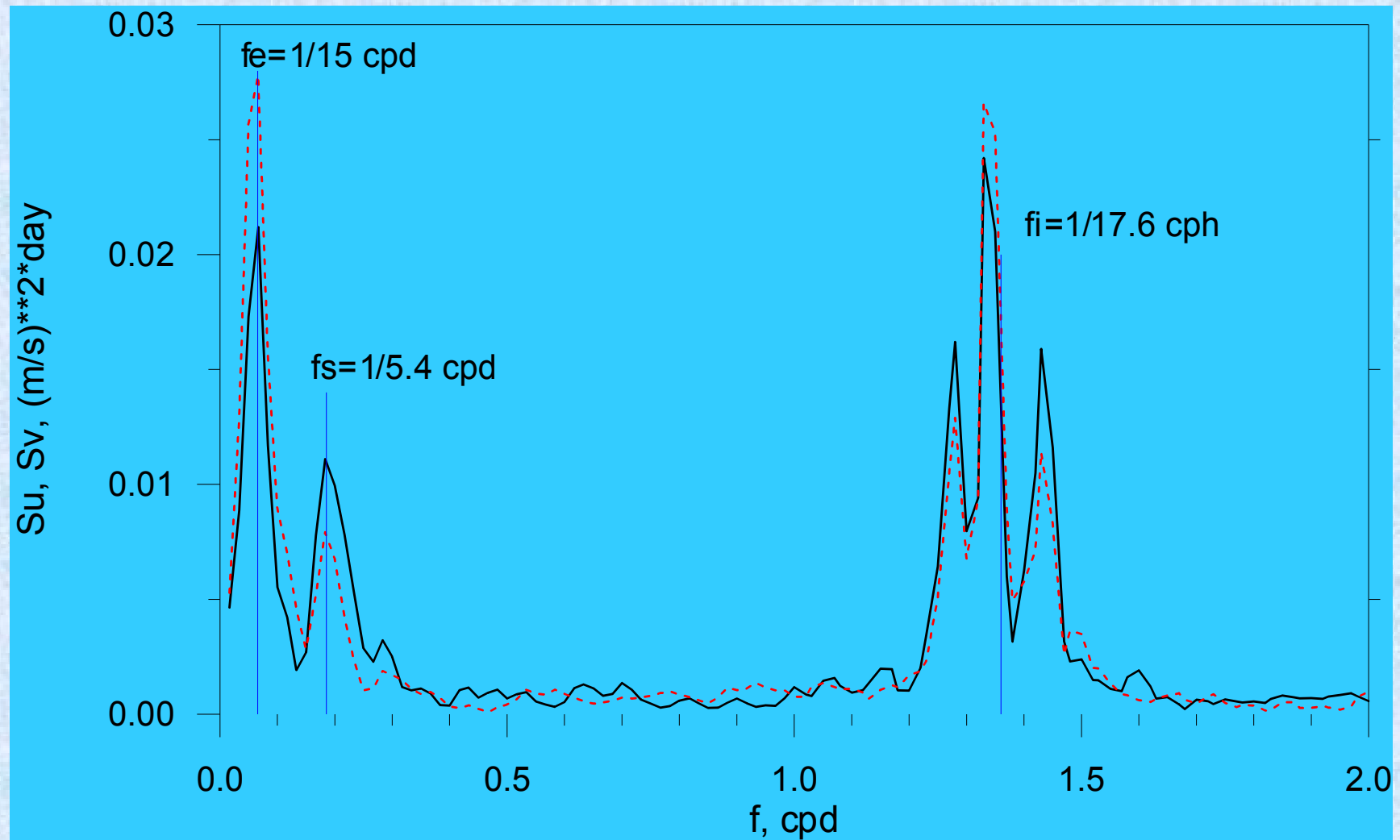
Example:

$$f=10^{-4} \text{ c}^{-1}, \quad V_i=30 \text{ cm/s} \quad \longrightarrow \quad R_i=3 \text{ km}$$

Manifestation of inertial oscillations at the Lagrangian drifter trajectory in the Black Sea



Power spectra of Lagrangian velocity components (Black Sea drifter experiment)



Ekman mass transport

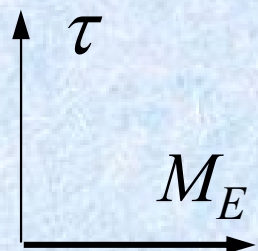
$$M_{Ex} = \int_{-H \gg H_E}^0 (\rho u) dz$$

$$M_{Ey} = \int_{-H \gg H_E}^0 (\rho v) dz$$

Using Ekman's solution for u and v , we obtain:

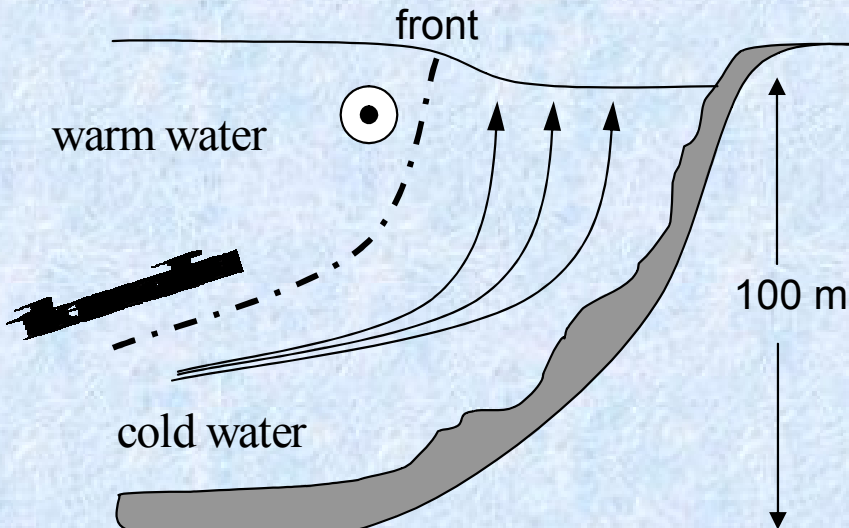
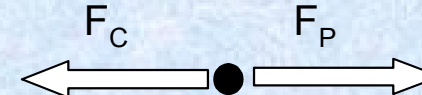
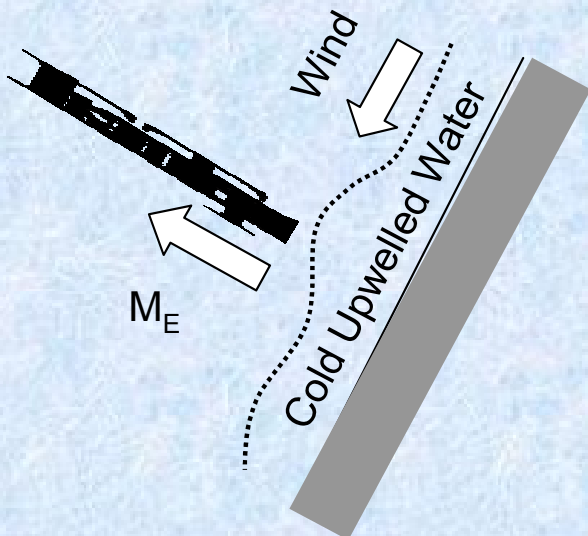
$$M_{Ex} = \frac{\tau_{yz}}{f} \quad M_{Ey} = -\frac{\tau_{xz}}{f} \quad M_E = \frac{(\tau \times k)}{f}$$

M_E - Ekman mass transport, directed to the right angle of wind stress in Northern Hemisphere

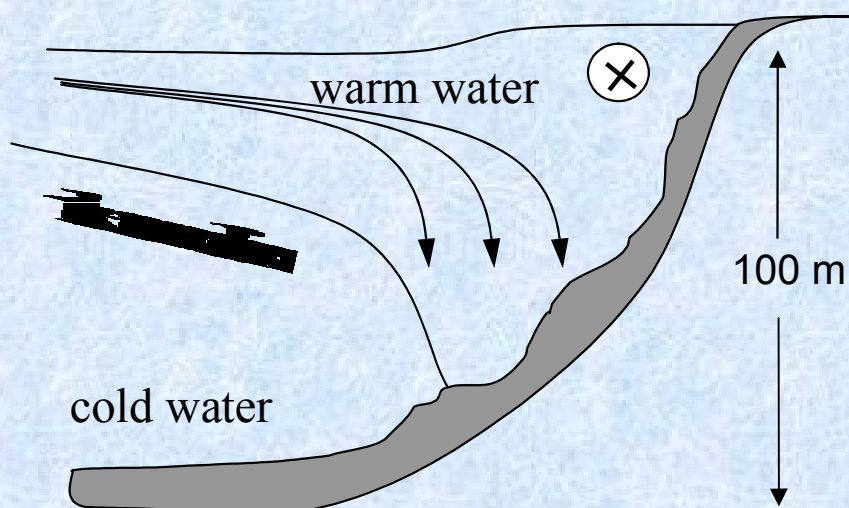
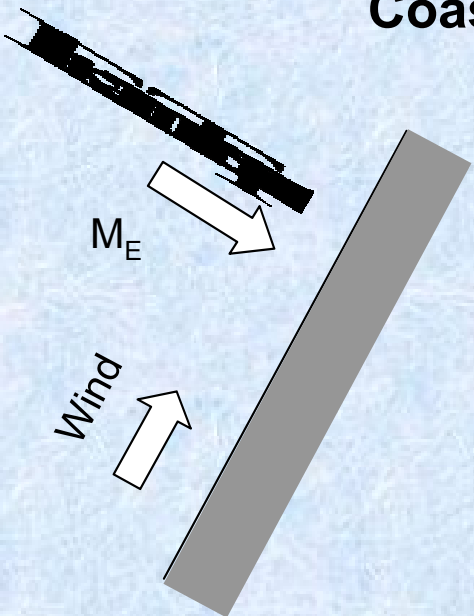


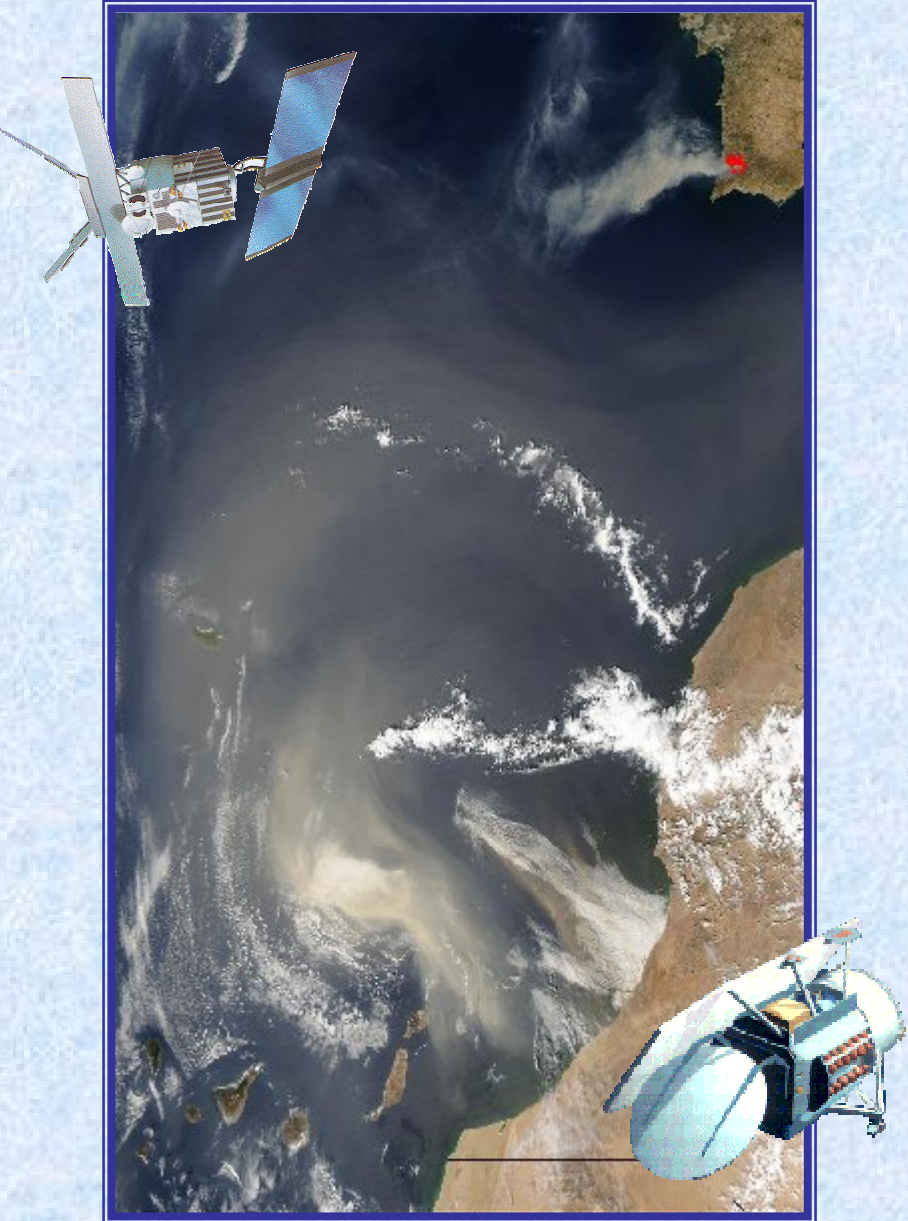
Wind induced nearshore circulation

Coastal upwelling



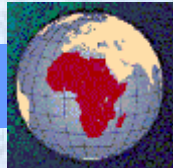
Coastal downwelling





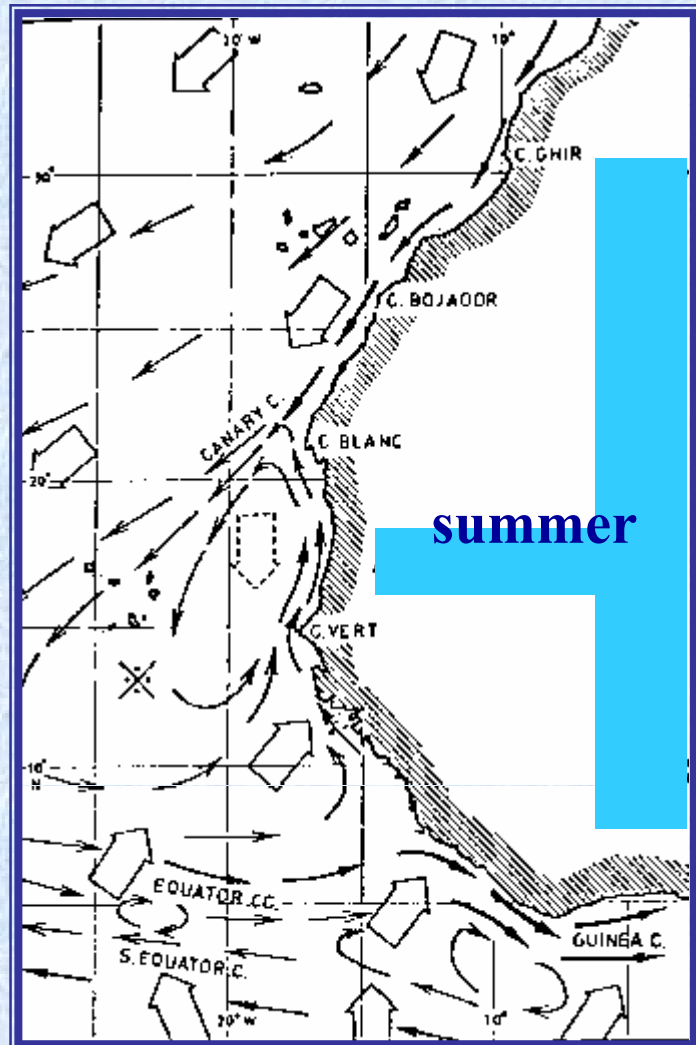
***Andrey G. Kostianoy
Sergey A. Lebedev
Alexander M. Sirota***

Canary Upwelling: Satellite Monitoring

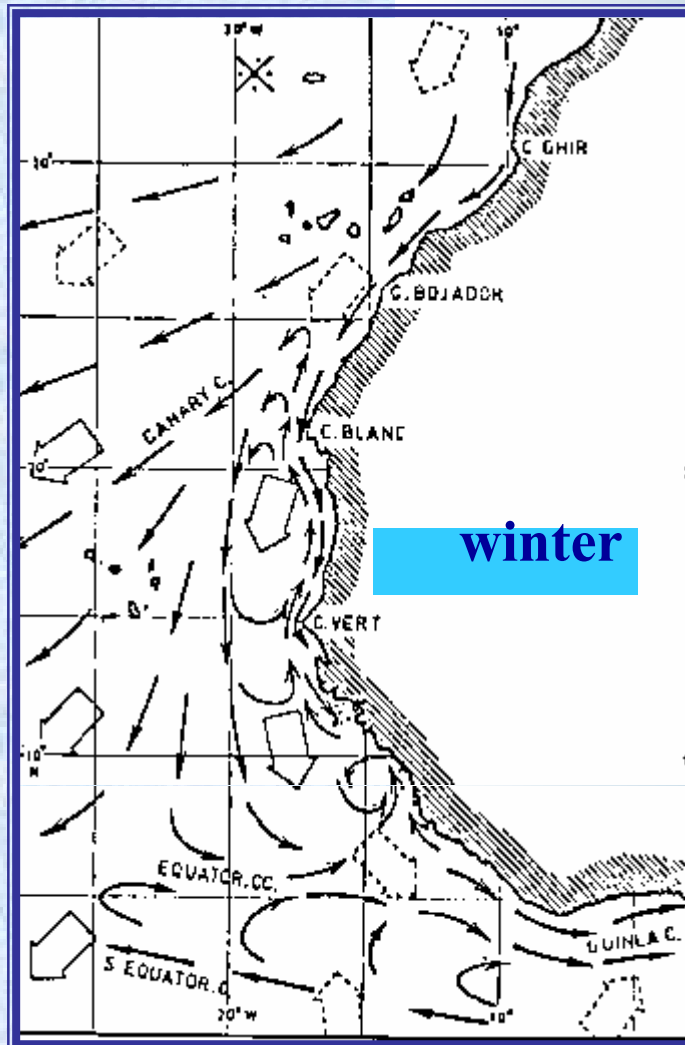


© 2004, Andrey G. Kostianoy, Sergey A. Lebedev, Alexander M. Sirota

Seasonal Circulation



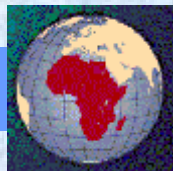
summer



winter

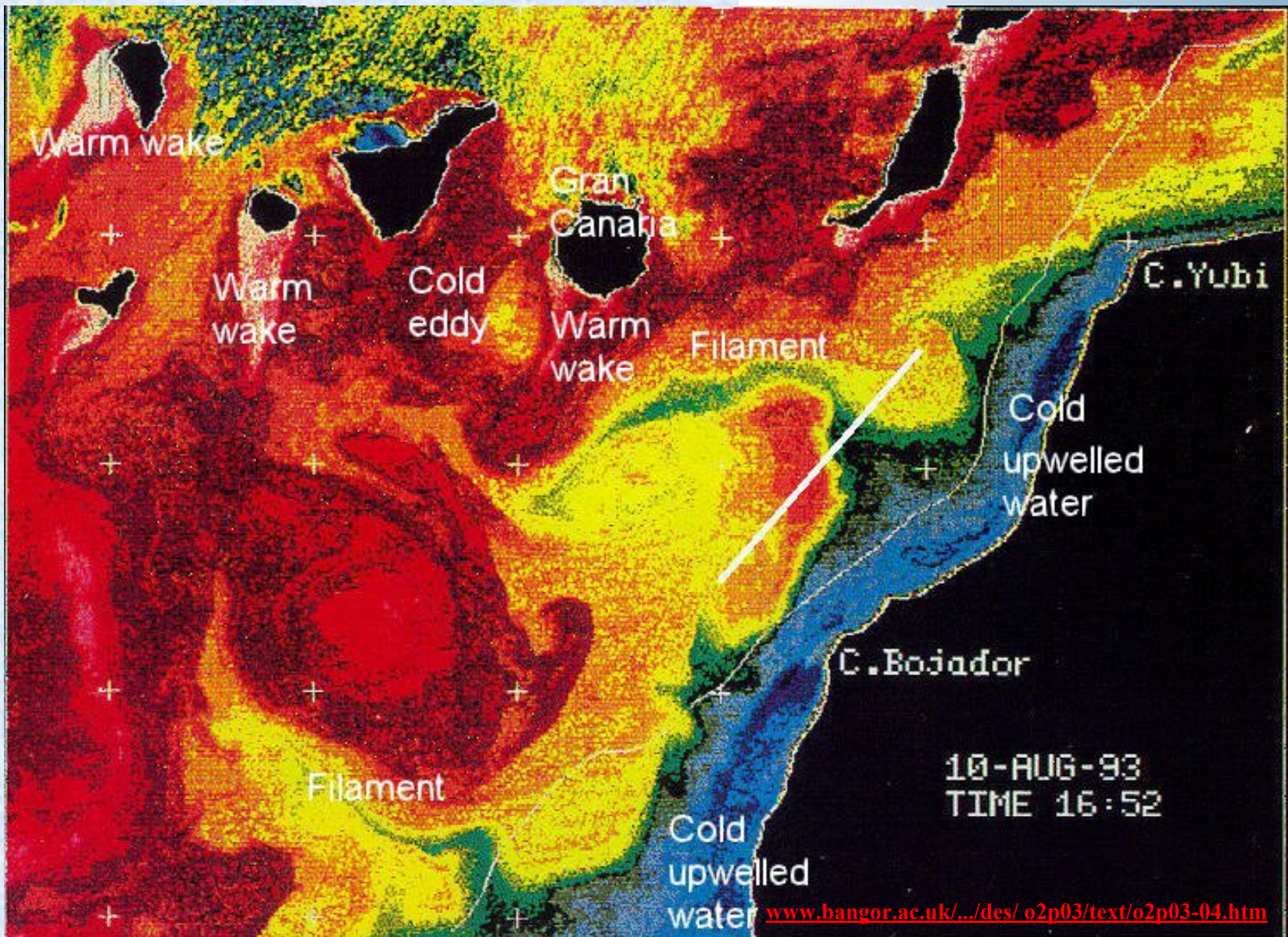
- dominating wind
- gentle and changeable winds
- regions of weak winds with variable direction
- sea surface currents

Mittellstaedt (1983)

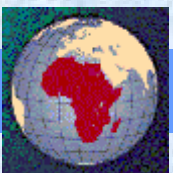


© 2004, Andrey G. Kostianoy, Sergey A. Lebedev, Alexander M. Sirota

Upwelling Features

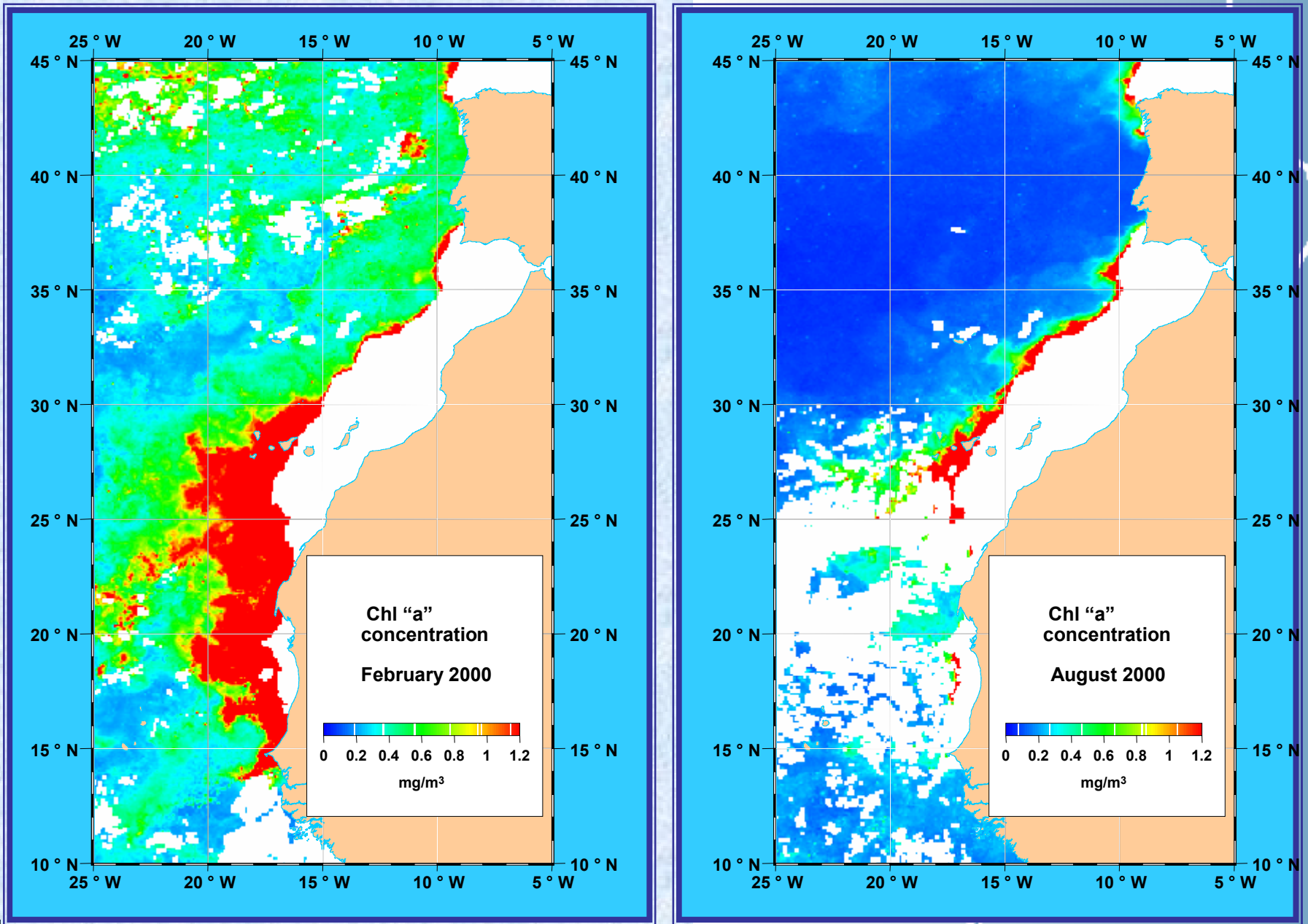


Des Barton



© 2004, Andrey G. Kostianoy, Sergey A. Lebedev, Alexander M. Sirota

Chl "a" concentration in February and August 2000



© 2004, Andrey G. Kostianoy, Sergey A. Lebedev, Alexander M. Sirota

Geostrophic balance

$$t \gg \frac{1}{f} : \quad \frac{du}{dt} = \frac{dv}{dt} = \frac{dw}{dt} = 0; A_z = 0$$

$$\frac{1}{\rho} \frac{\partial p}{\partial x} = fv \quad v = \frac{1}{f\rho} \frac{\partial p}{\partial x}$$

$$v = \frac{1}{f\rho} \frac{\partial}{\partial x} \int_{-H}^0 g\rho(z) dz - \frac{g}{f} \frac{\partial \zeta}{\partial x}$$

$$\frac{1}{\rho} \frac{\partial p}{\partial y} = -fu \quad u = -\frac{1}{f\rho} \frac{\partial p}{\partial y}$$

$$u = -\frac{1}{f\rho} \frac{\partial}{\partial y} \int_{-H}^0 g\rho(z) dz - \frac{g}{f} \frac{\partial \zeta}{\partial y}$$

$$\frac{1}{\rho} \frac{\partial p}{\partial z} = -g \quad p = p_a + \int_{-H}^{\zeta} g\rho(z) dz$$

$$u_s = -\frac{g}{f} \frac{\partial \zeta}{\partial y} \quad v_s = \frac{g}{f} \frac{\partial \zeta}{\partial x}$$

Example:

$$f=10^{-4} \text{ s}^{-1}, \quad g=10^3 \text{ cm/s}^2, \quad \frac{\partial \zeta}{\partial y} = 3 \text{ cm/10 km} \quad \Longrightarrow \quad u_s = 30 \text{ cm/s}$$

Wind stress vorticity as a driving mechanism of basinscale circulation in seas

$$\frac{\partial}{\partial x}(M_{Ex}) + \frac{\partial}{\partial y}(M_{Ey}) = \frac{1}{f} \left[\frac{\partial \tau_{yz}}{\partial x} - \frac{\partial \tau_{xz}}{\partial y} \right] = \frac{\text{curl } \tau}{f}$$

$$\frac{\partial}{\partial x}(M_{Ex}) + \frac{\partial}{\partial y}(M_{Ey}) = -\rho w_E$$

$$w_E = \frac{\text{curl } \tau}{f\rho} \quad \text{- Ekman pumping velocity}$$

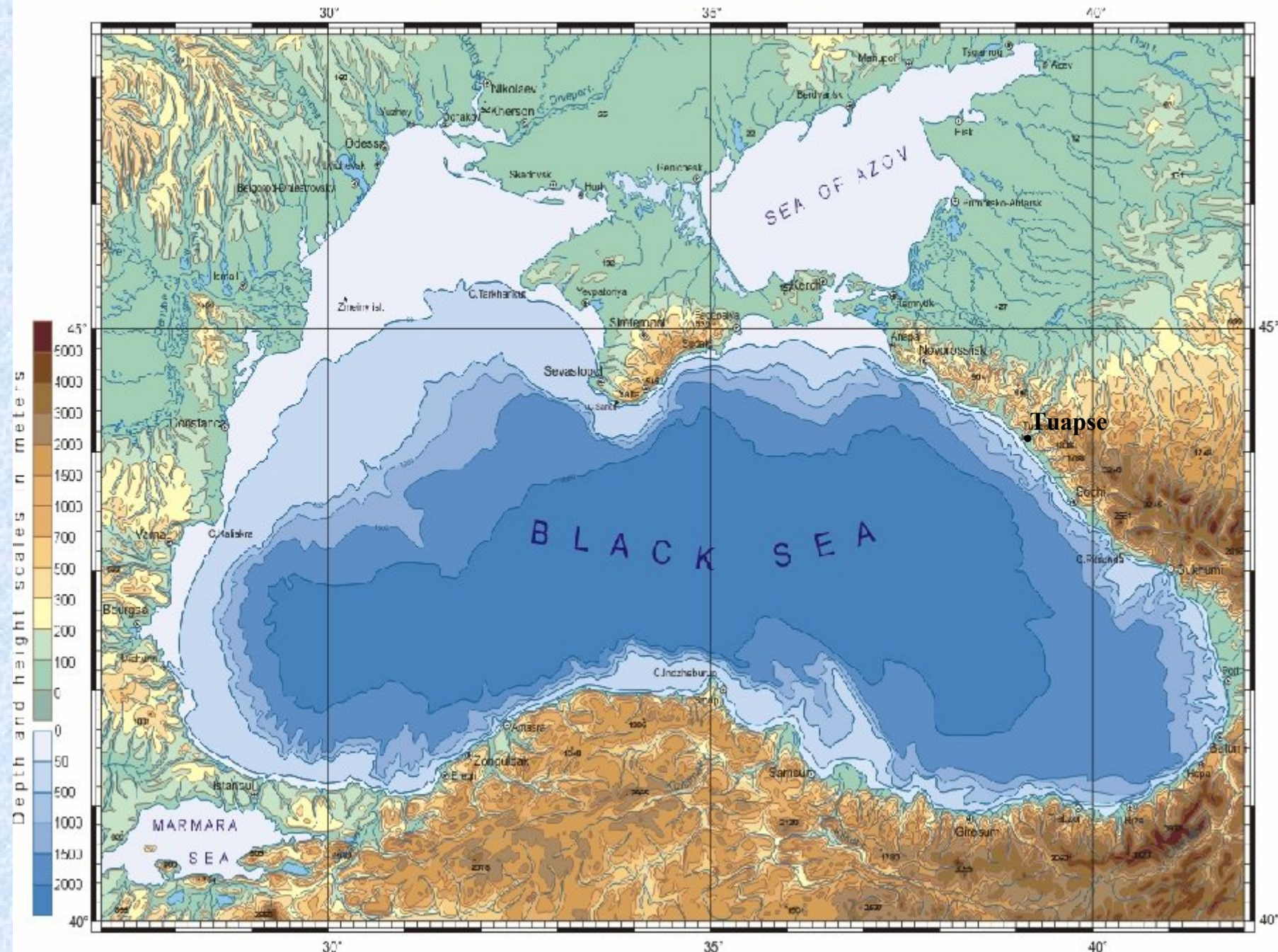
Predominantly positive (negative) wind stress vorticity at the sea surface area produces the divergence of Ekman mass transport and associated upwelling (downwelling). As a result horizontal pressure gradients (related to the elevation of sea level and isopycnal surfaces) appear and the basinscale geostrophic currents are generated.

Baroclinic instability of currents, formation of meanders and mesoscale eddies

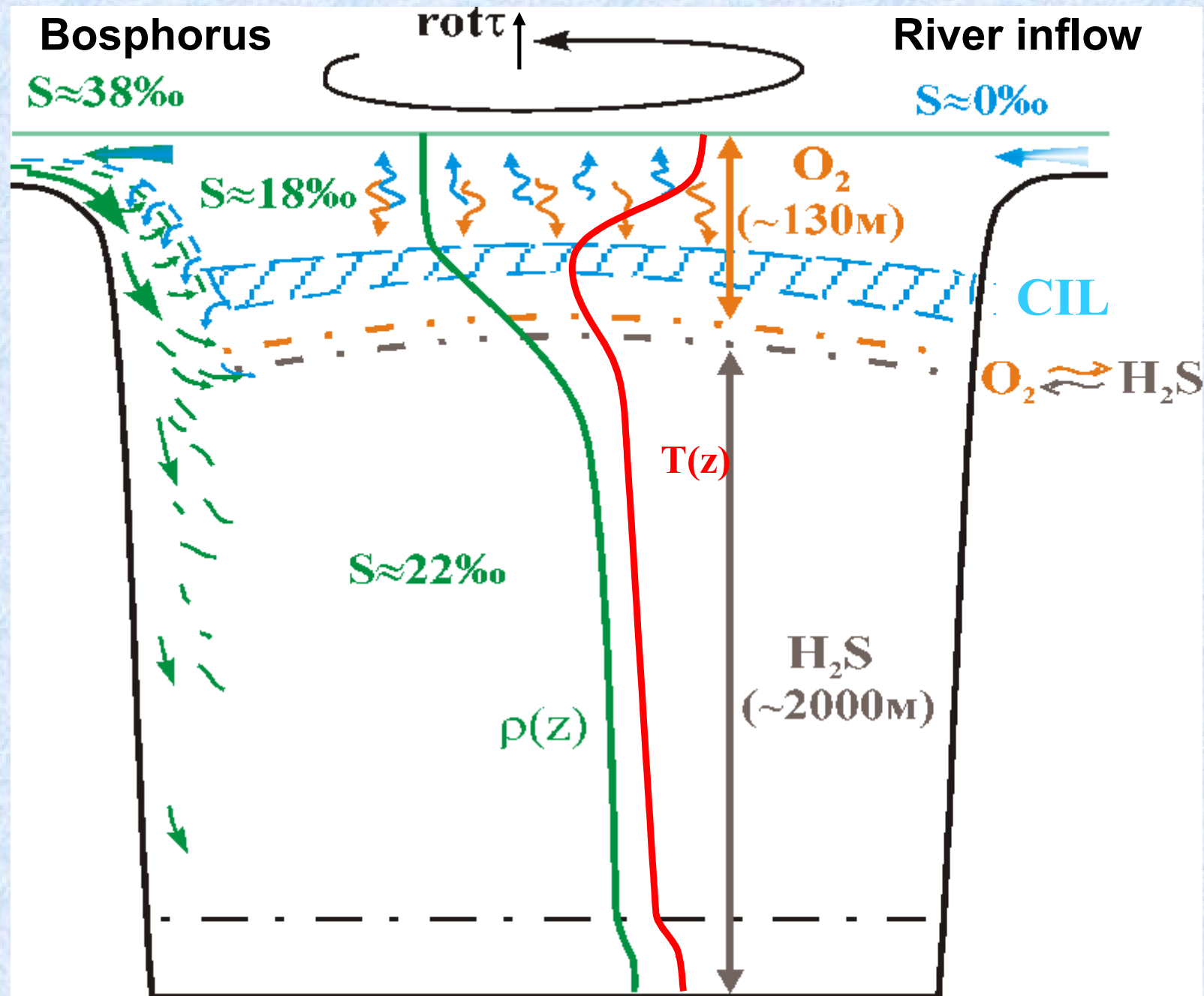
Nearly geostrophic currents in stratified ocean in many cases are unstable. Two types of instability are widespread: barotrophic (related to the horizontal shear of the flow) and baroclinic (related to the vertical shear of the flow). Due to the baroclinic instability flow becomes meandering. Sometimes meanders are growing to high amplitude. In these cases they could be transformed into mesoscale eddies which “break” the basic flow and produce an intensive horizontal mixing. The necessary condition for the development of baroclinic instability is $L \gg R_d$, where L is the width of the flow and $R_d = NH/f$ – the baroclinic deformation radios. The typical wave length of meander $\lambda \approx 2\pi R_d$ and the radios of mesoscale eddy $R_e \approx \pi R_d$.

Studies of wind forcing impact on basinscale currents, mesoscale eddy dynamics and the interaction between the coastal zone and the deep basin in the Black Sea.

BLACK AND AZOV SEAS

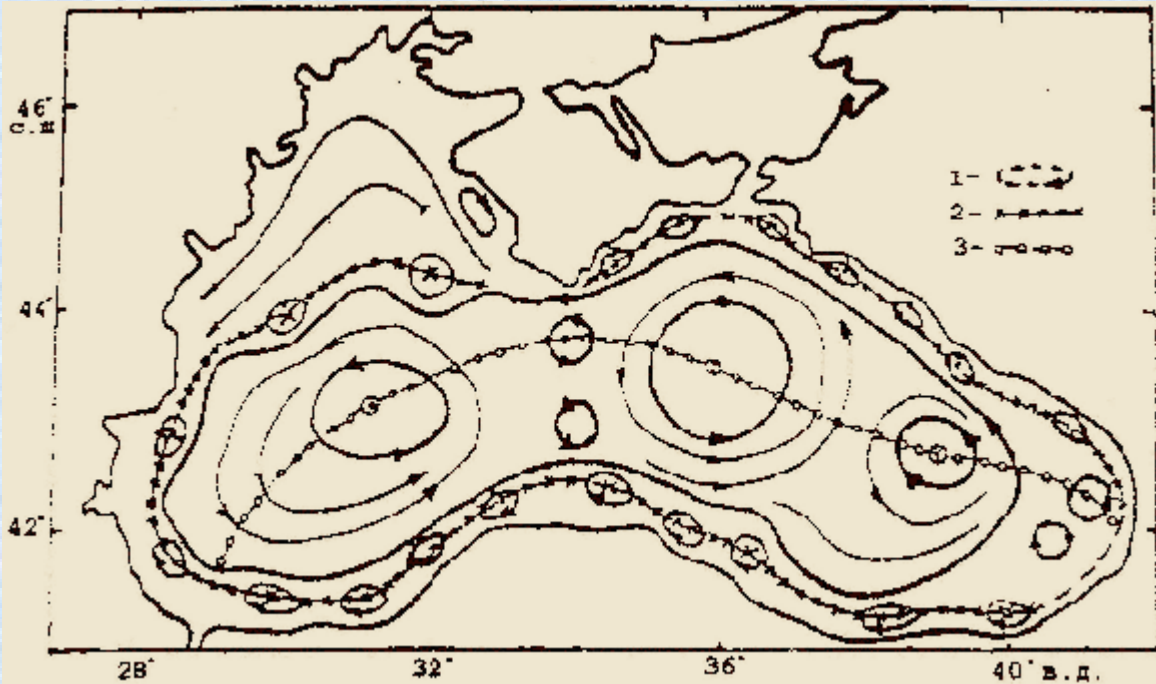


Black Sea hydrological structure

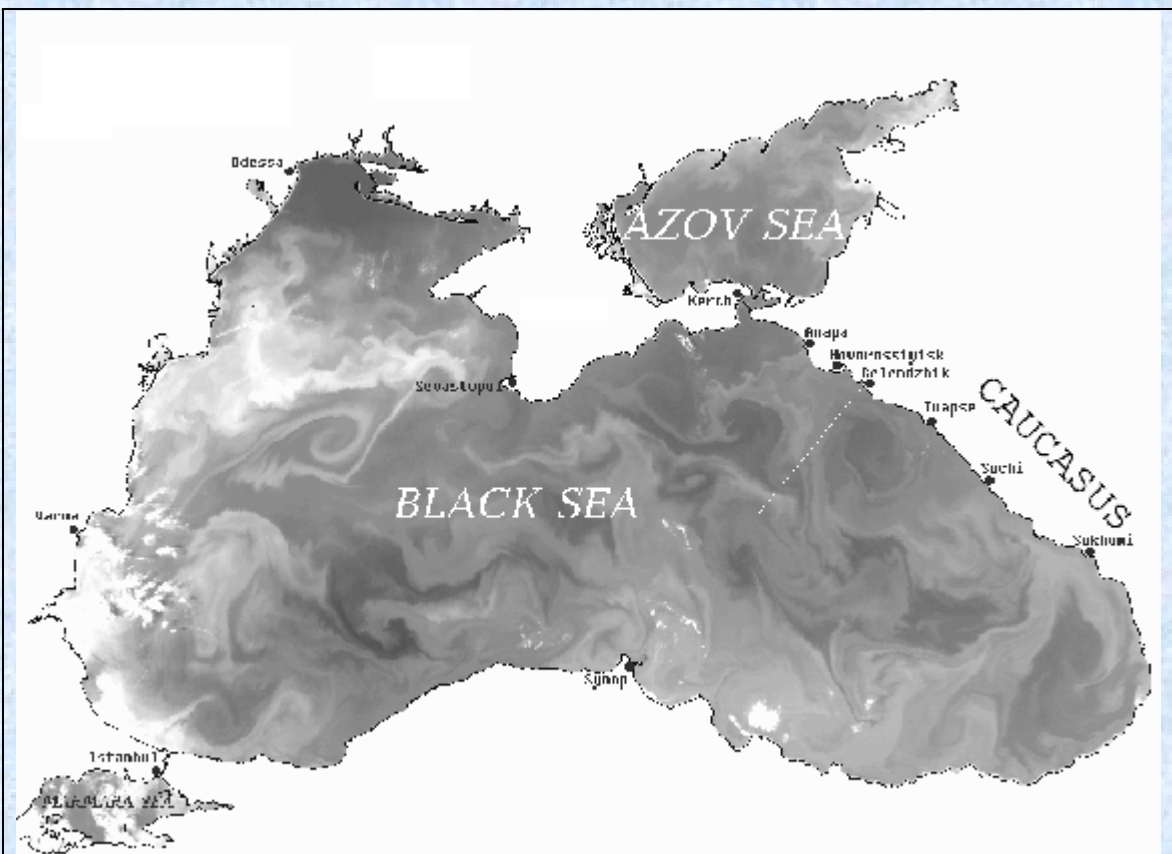


The scheme of the Black Sea upper layer circulation

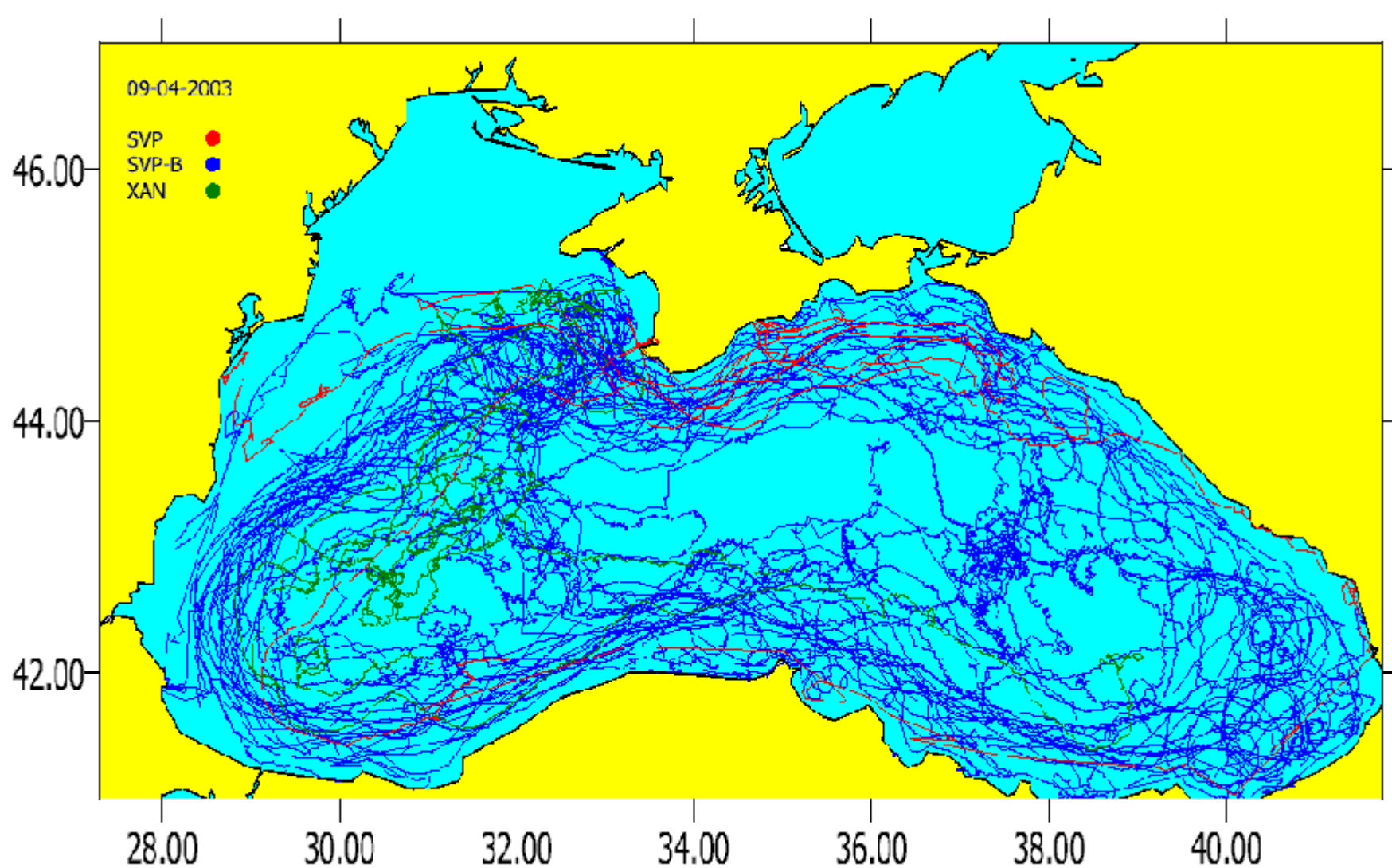
(Ovchinnikov and Popov, 1990)



Satellite image of mesoscale eddy structures in the Black Sea



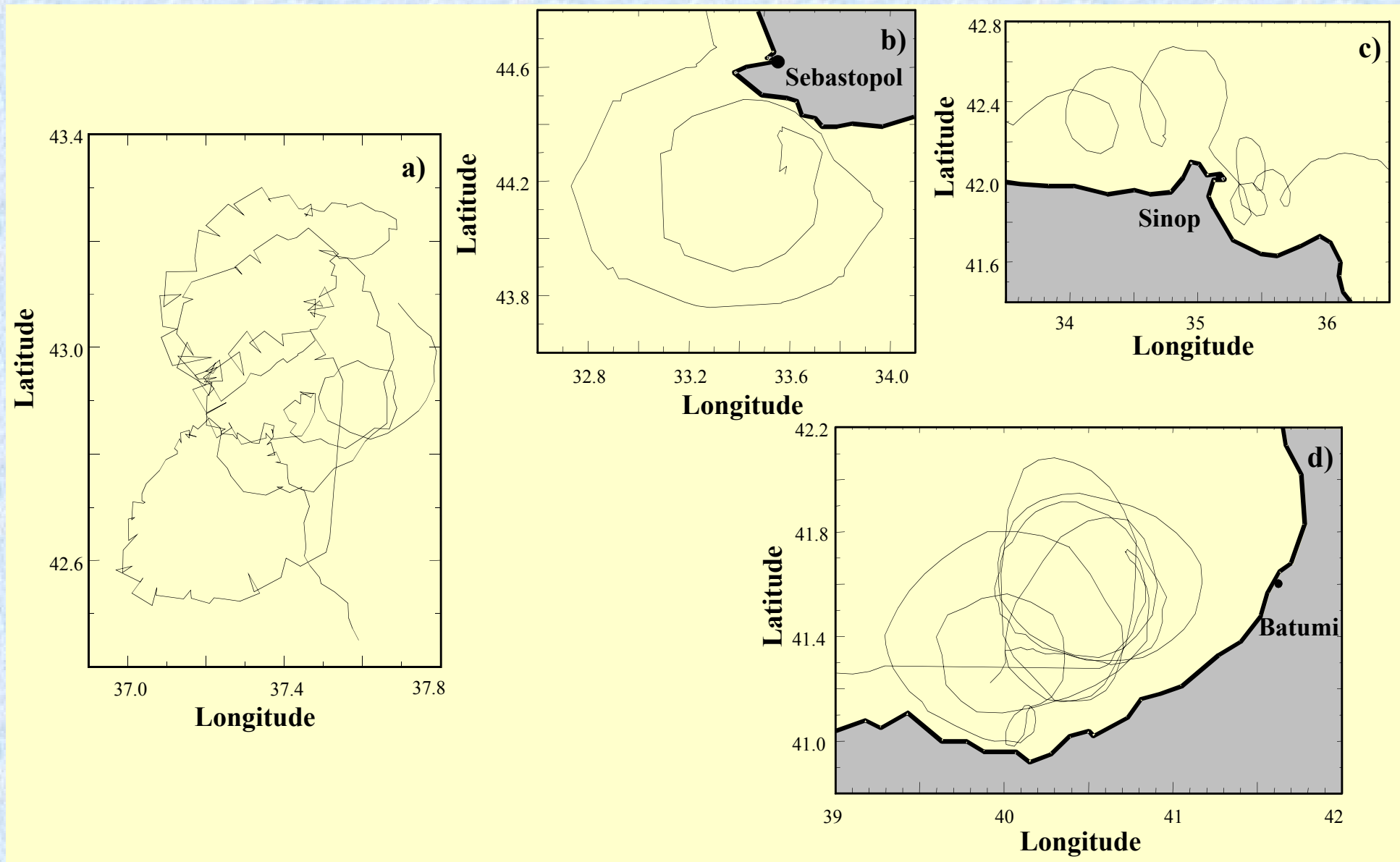
International Black Sea drifter experiment 1999-2003



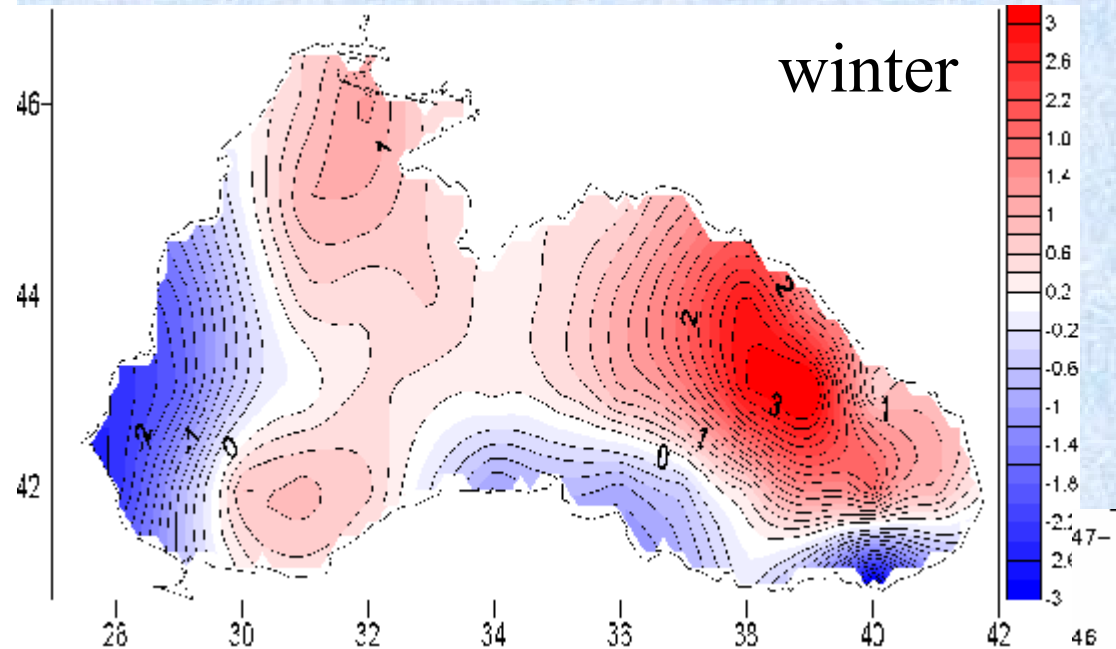
Zhurbas, Zatsepin et al., 2004;

Poulain, Barbatini, Motyzhev, Zatsepin, 2005.

Fragments of trajectories of drifters trapped by eddies



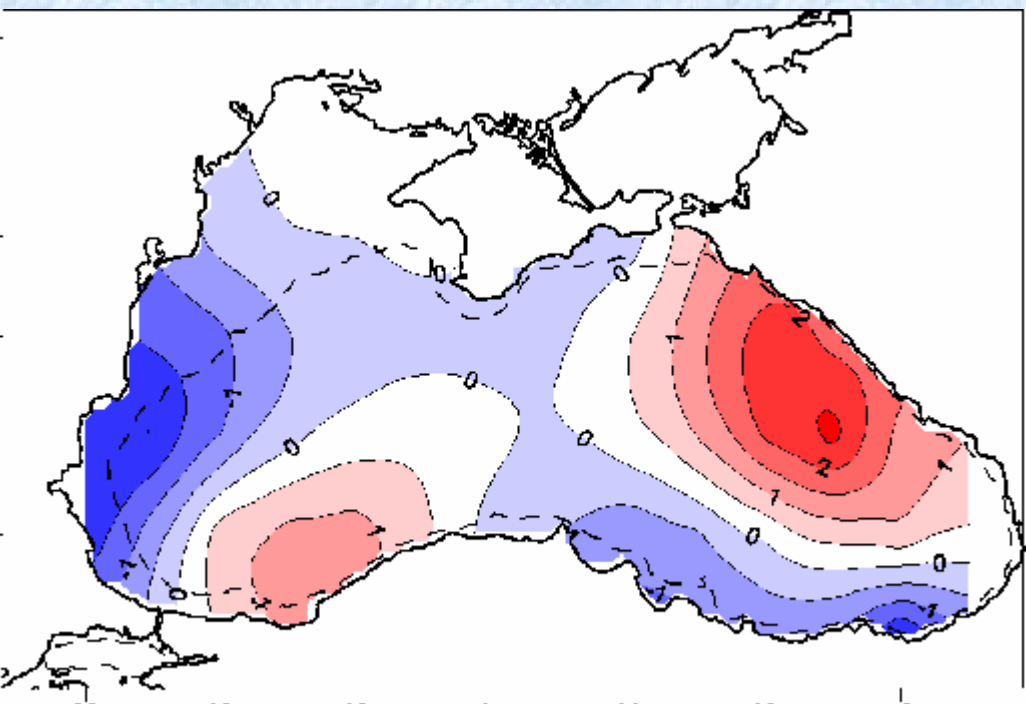
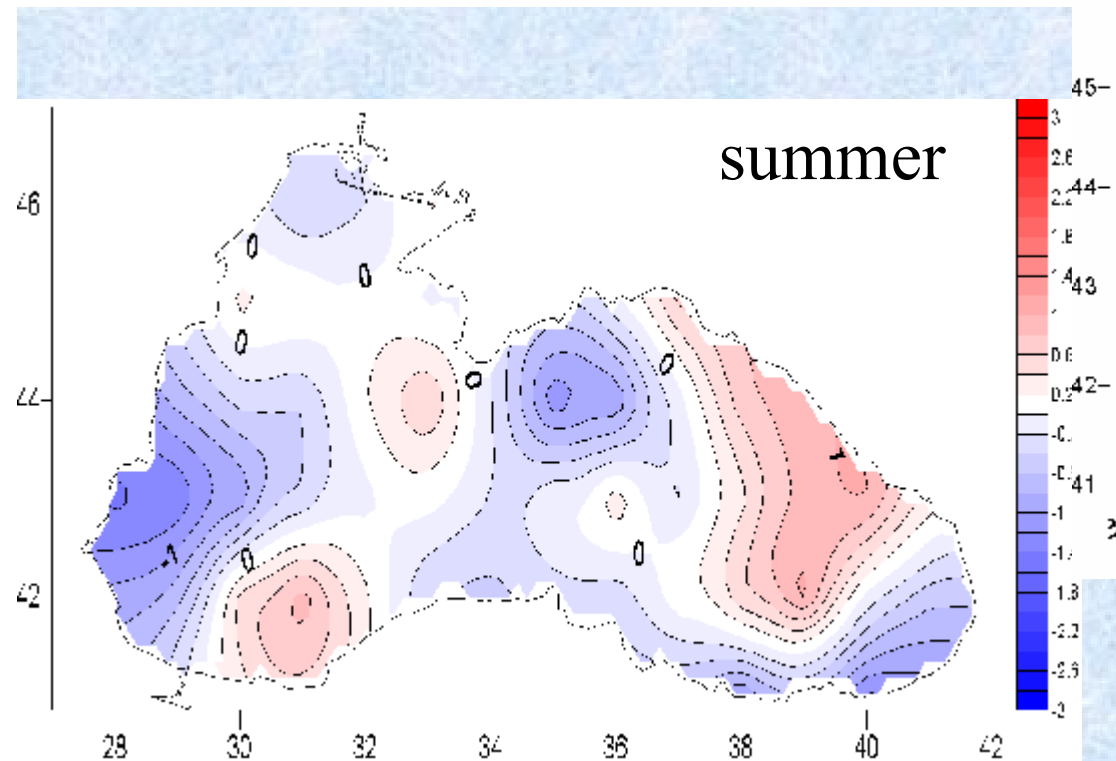
Ekman pumping velocity ($W_E 10^6 \text{ m/s}$) distribution



$$-\nabla_H M_E / \rho_w = W_E = \text{curl} \tau / (\rho f)$$

Positive values (red) – cyclonic
wind vorticity.

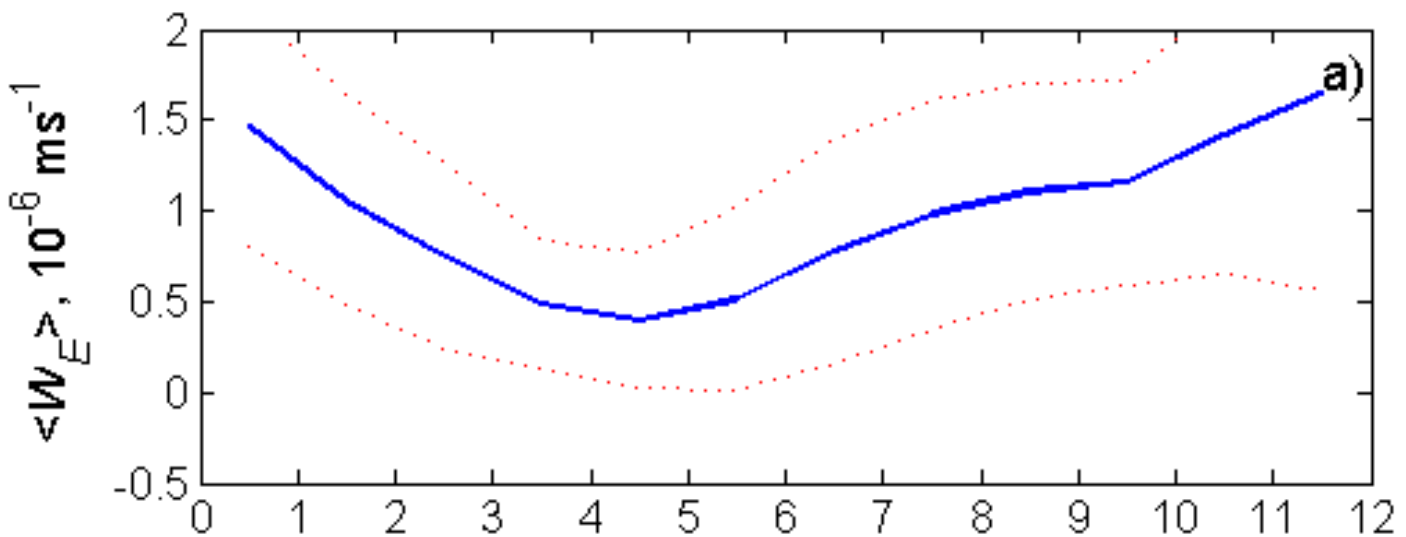
Negative values (blue) –
anticyclonic wind vorticity.



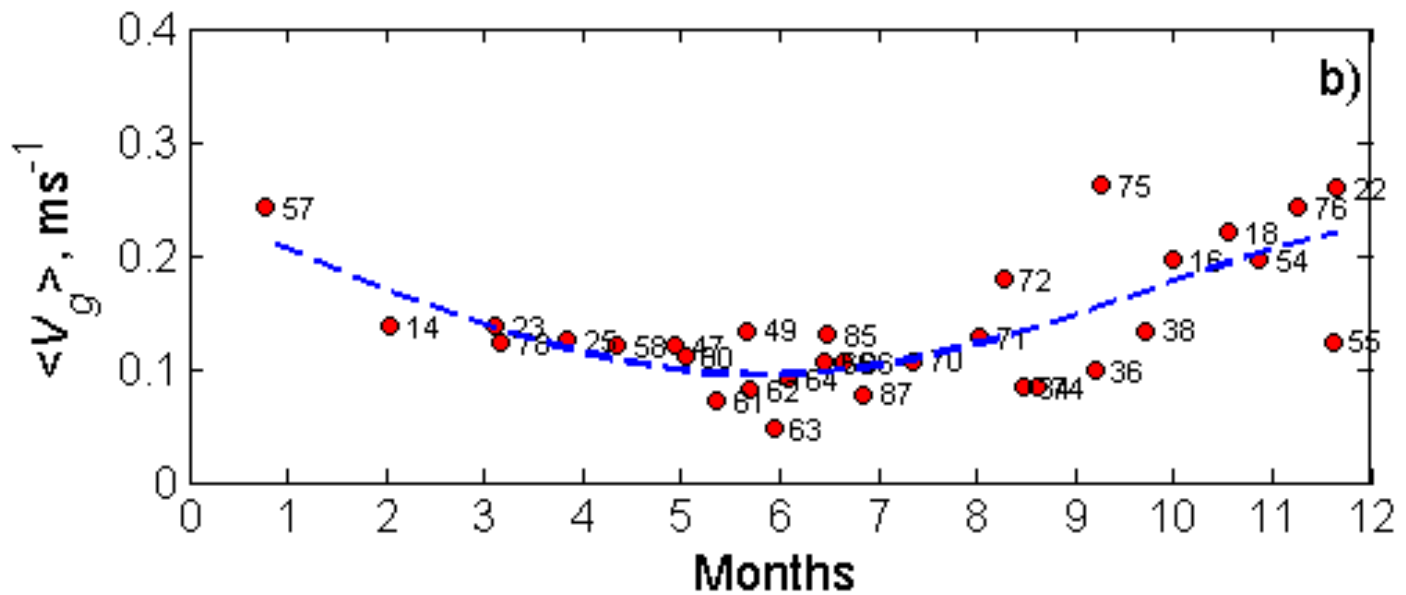
averaged over 7 years period
(1998-2004)

Within-year variability of $\langle W_E \rangle$ and $\langle V_g \rangle$ in the NE Black Sea

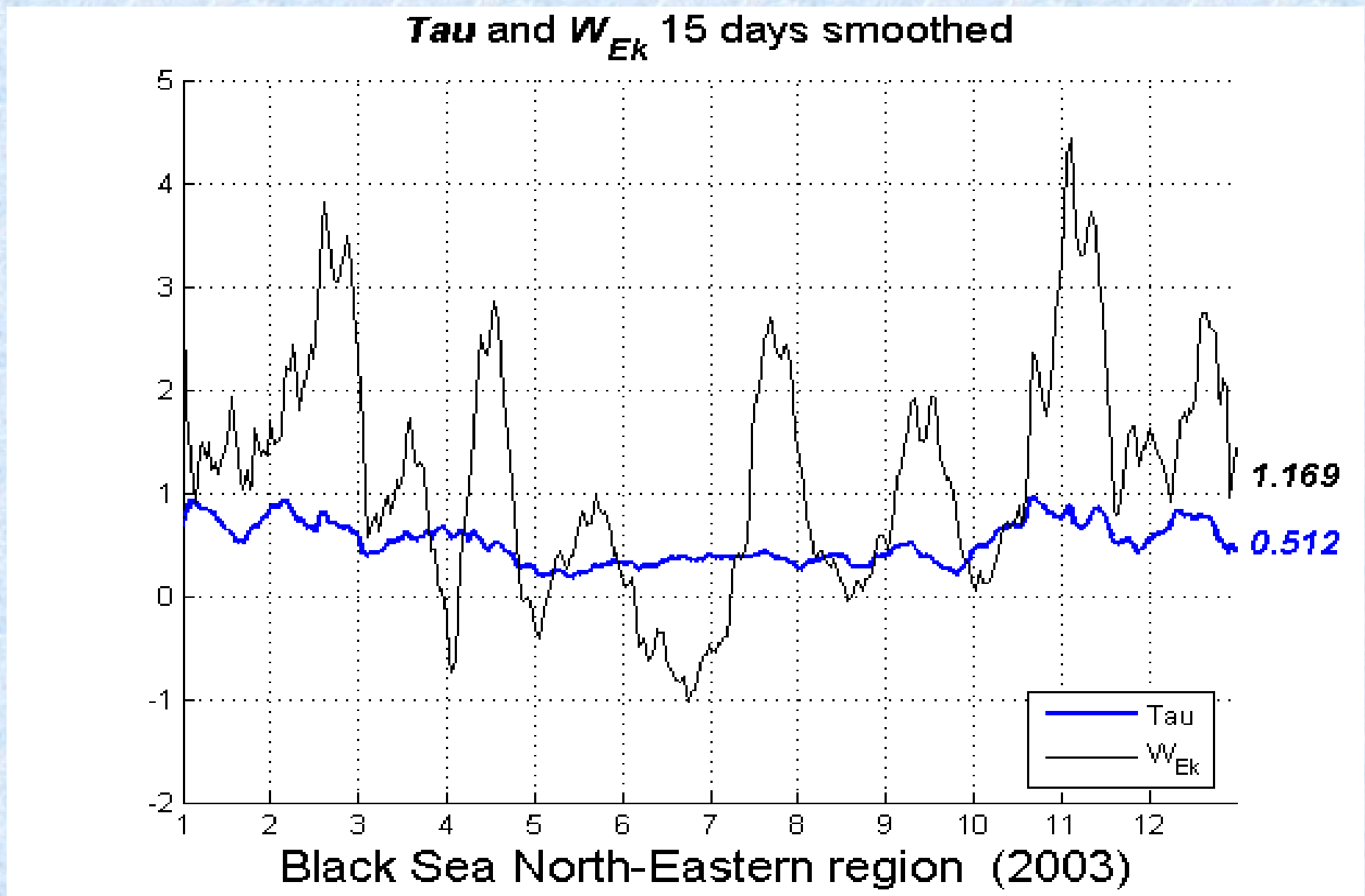
Ekman pumping
velocity



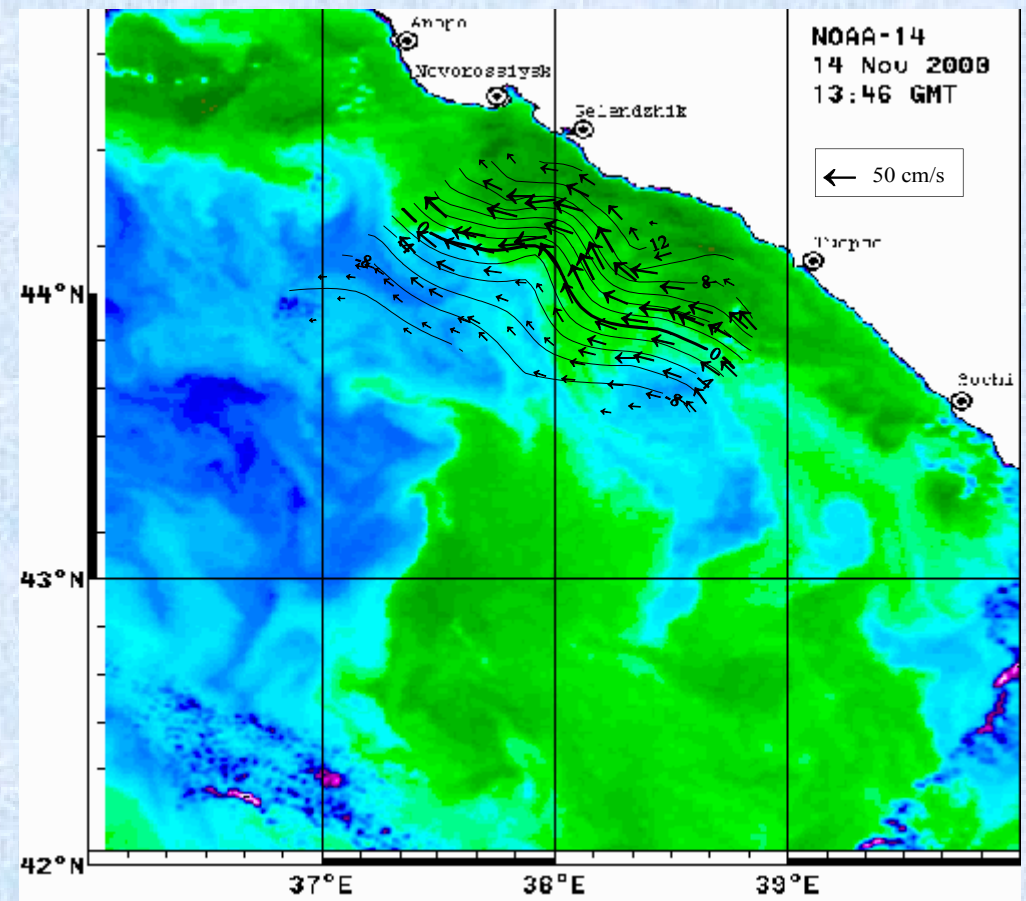
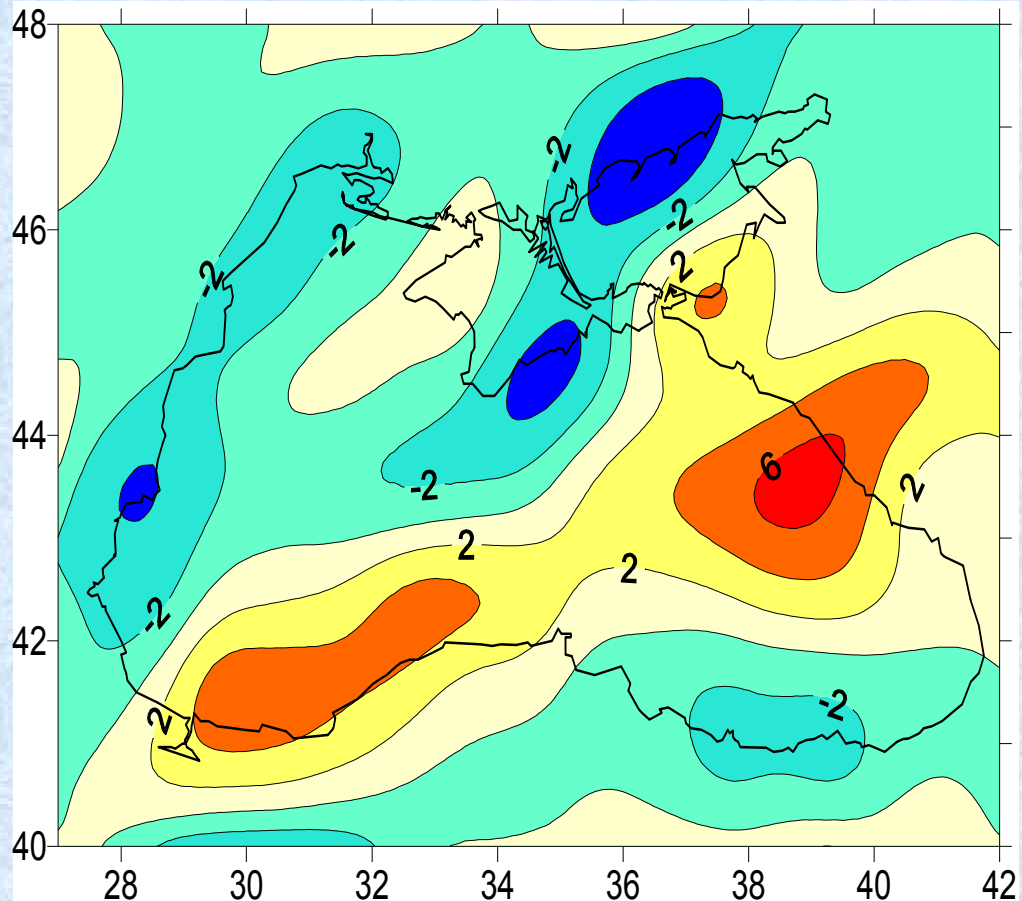
Mean alongshore
surface geostrophic
velocity



Intra-annual variability of wind stress (blue) and Ekman pumping velocity (black)

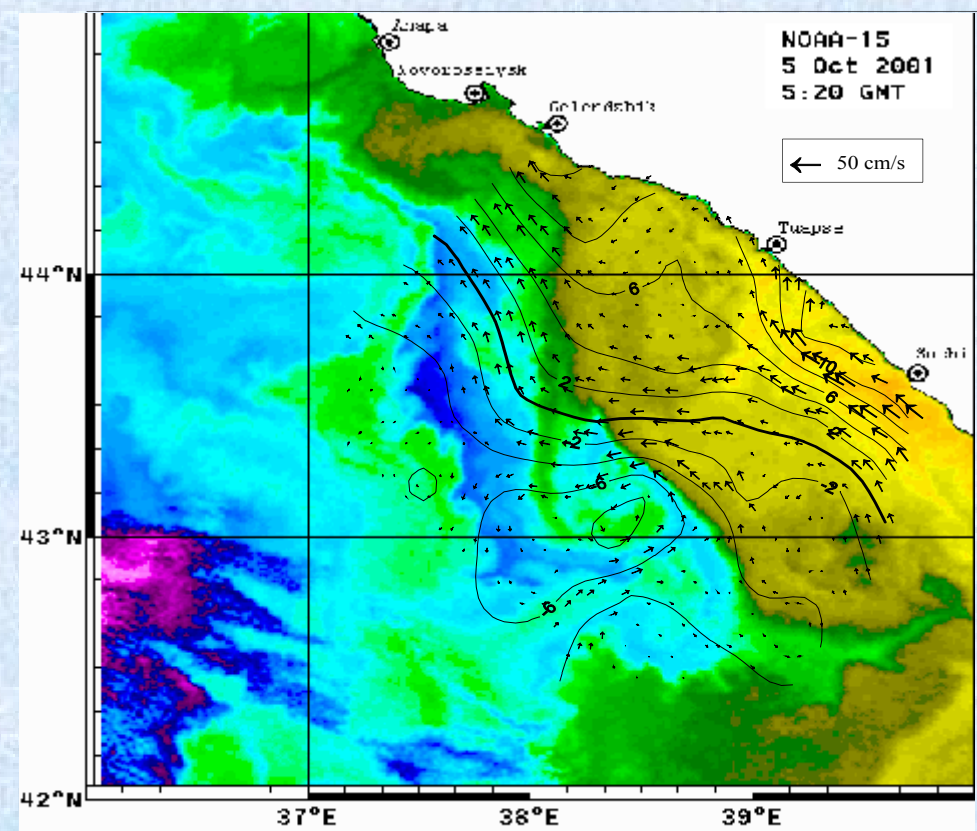
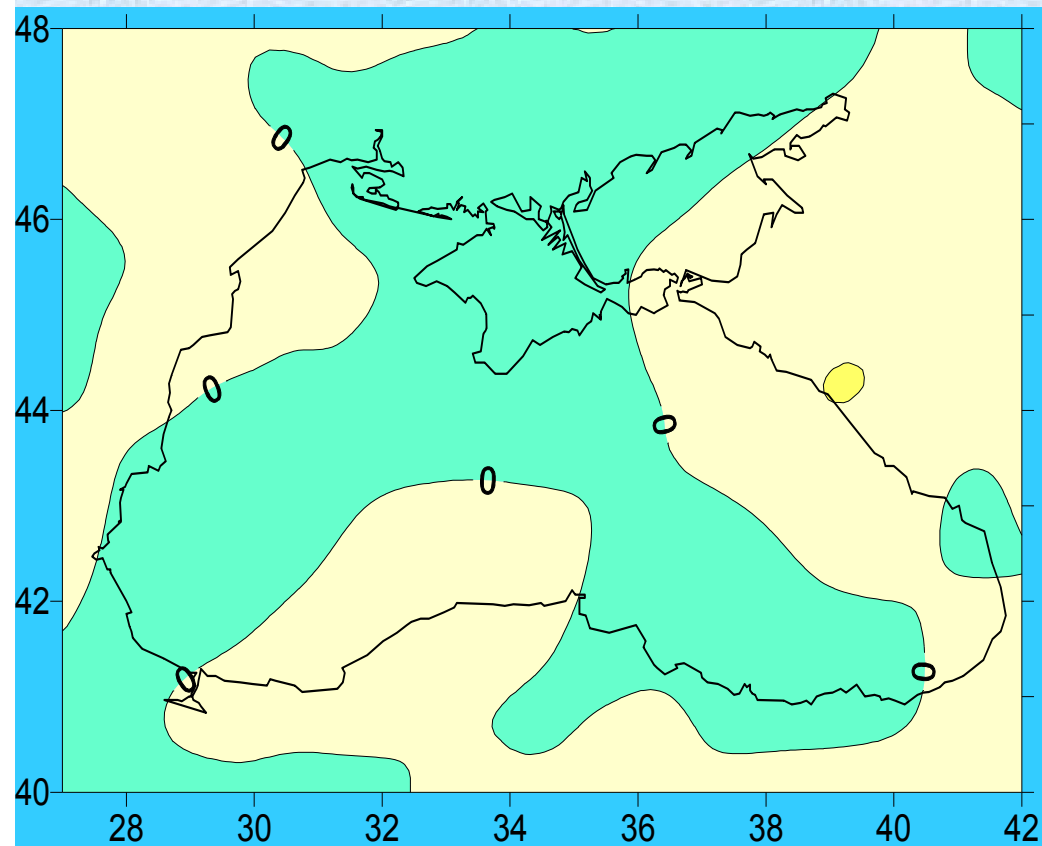


The high level of Ekman pumping causes intensification of the Rim current (November 2000)



Zatsepin et al., 2002

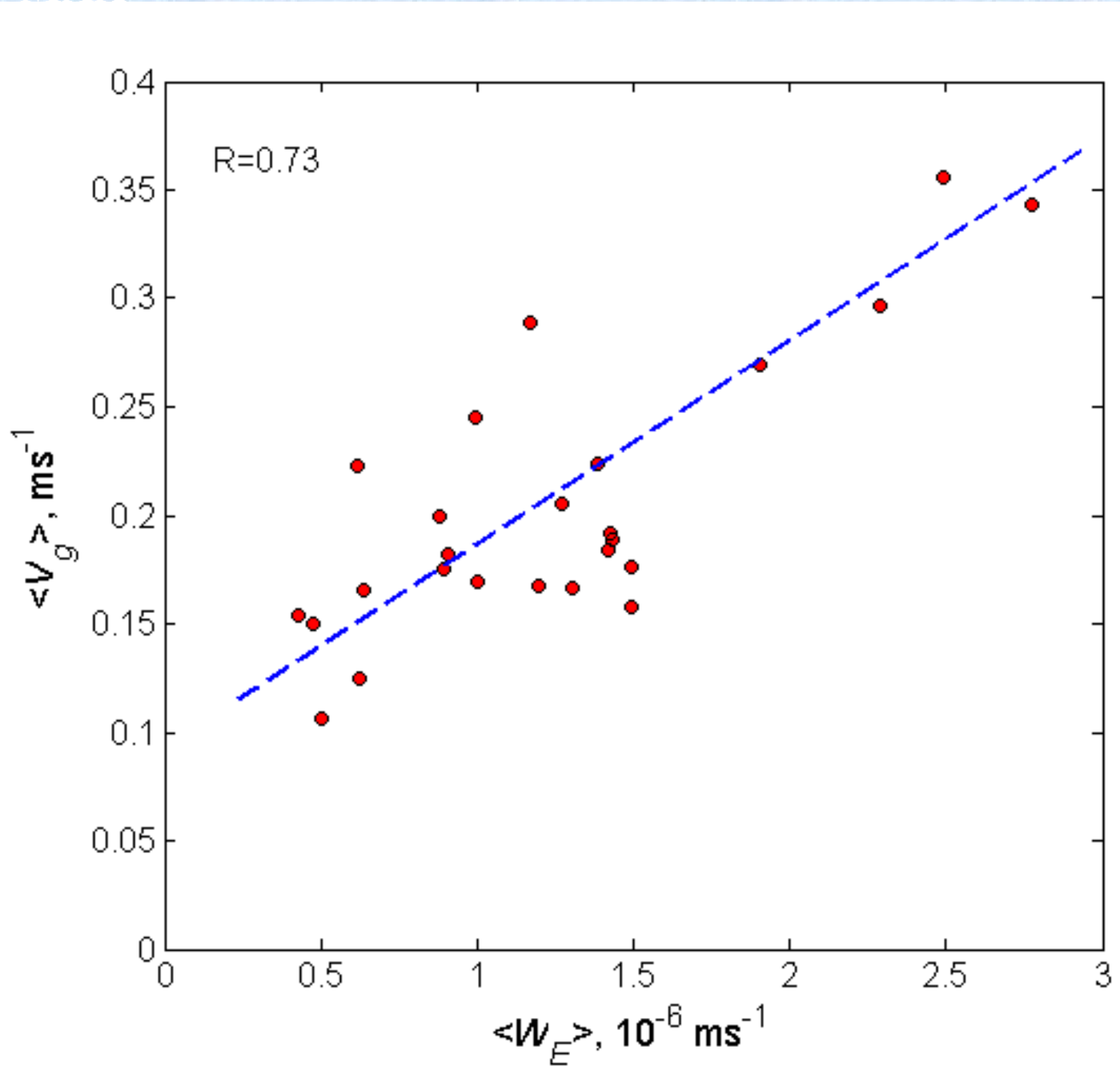
The low level of Ekman pumping causes the Rim current instability and degradation. Meanwhile eddy dynamics and lateral mixing increase (October 2001)



Zatsepin et al., 2002

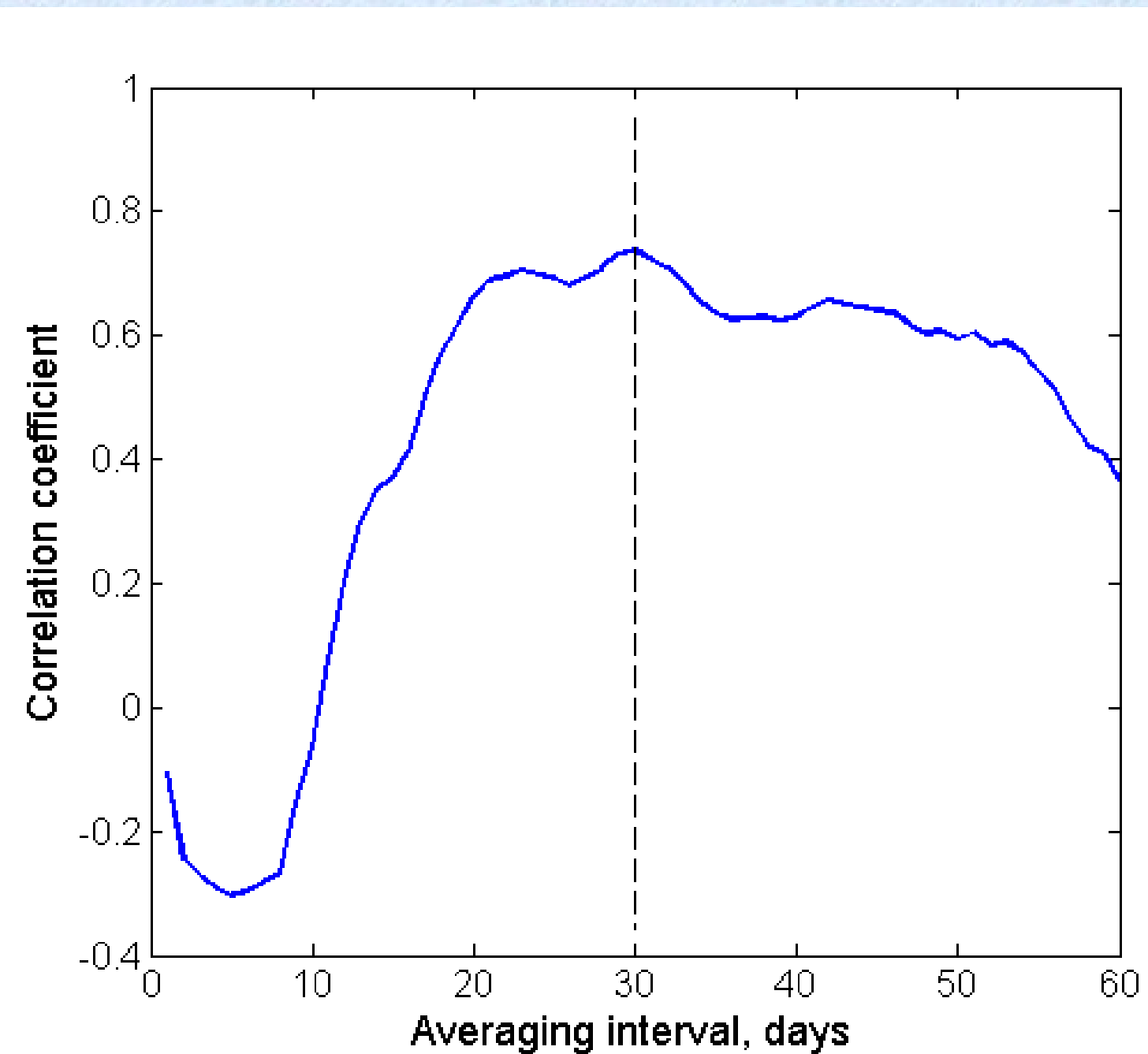
Surface geostrophic velocity in the Rim current core (V_{MAX}) as a function of $\langle W_E \rangle$

The maximal velocity in the Rim current is positively correlated with Ekman pumping velocity



Correlation coefficient between the V_{\max} and the $\langle W_E \rangle$ as a function of time averaging interval

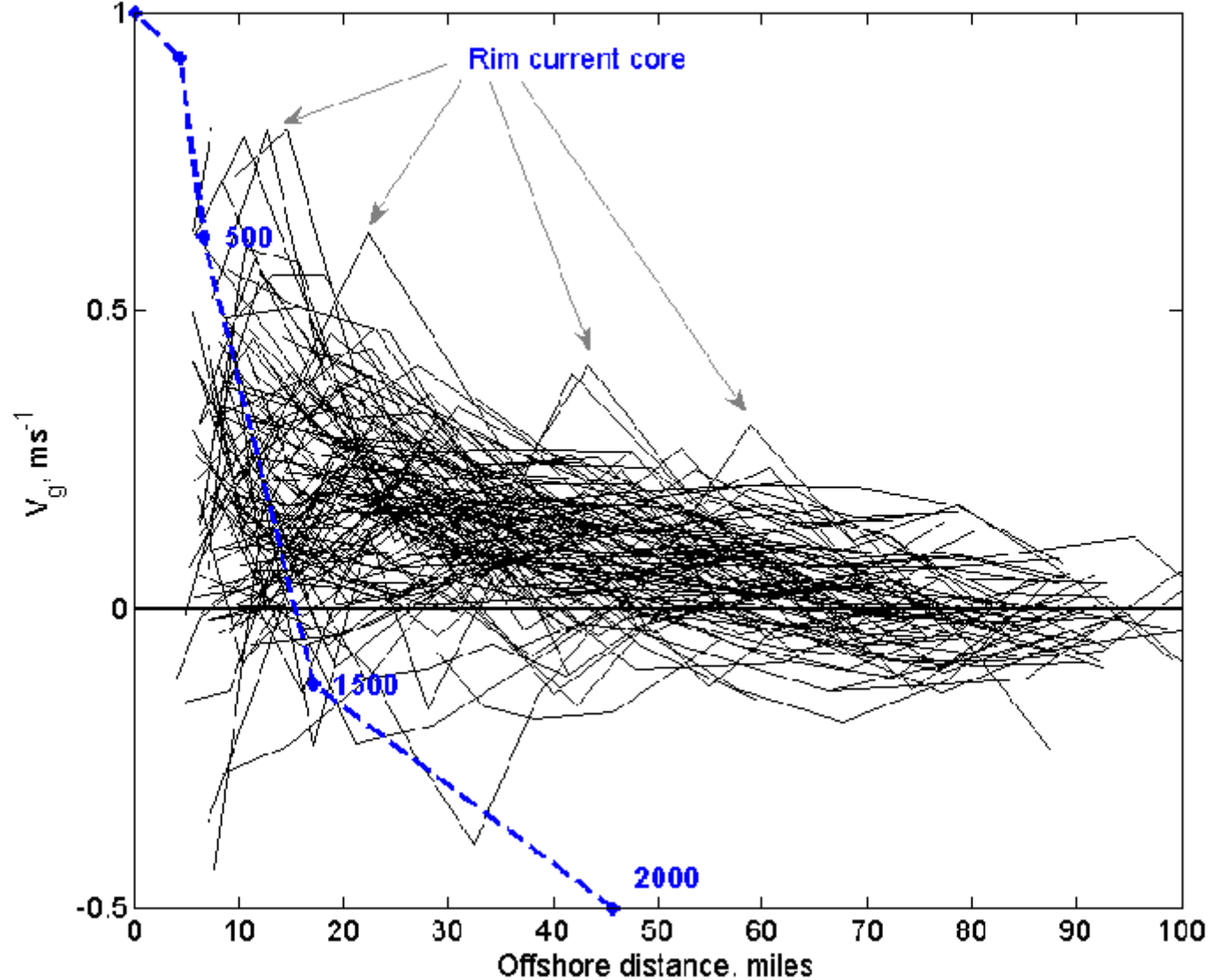
The correlation coefficient between the V_{\max} and the $\langle W_E \rangle$ peaks when the averaging time interval equals to 20-30 days before the observations



Alongshore surface geostrophic velocity distribution in the north-eastern part of Black Sea (dashed line - continental slope)

The Rim current is not topographically controlled in the north-eastern part of the Black Sea

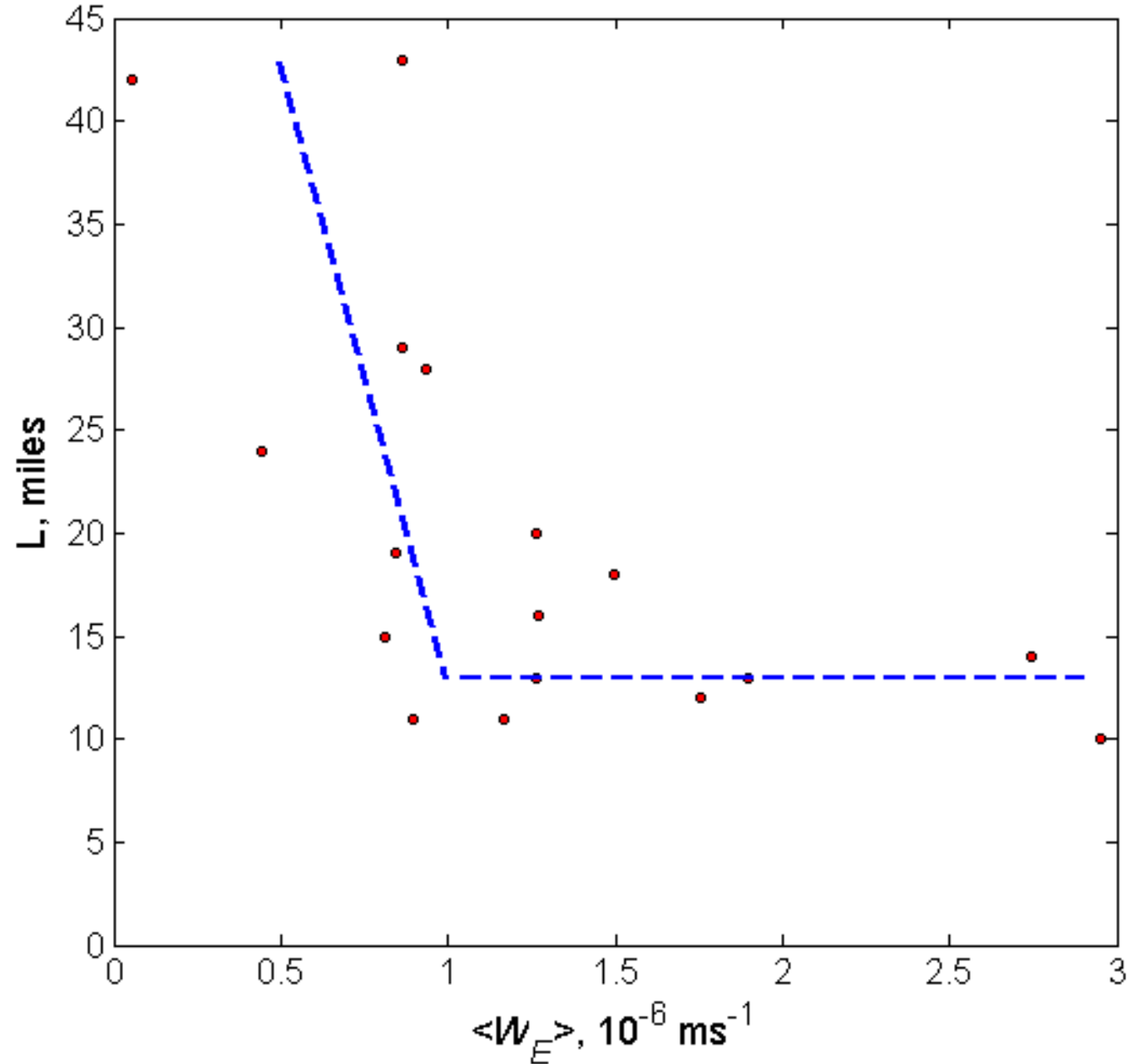
Maximal velocity in the Rim current core is observed when the jet is located over the continental slope



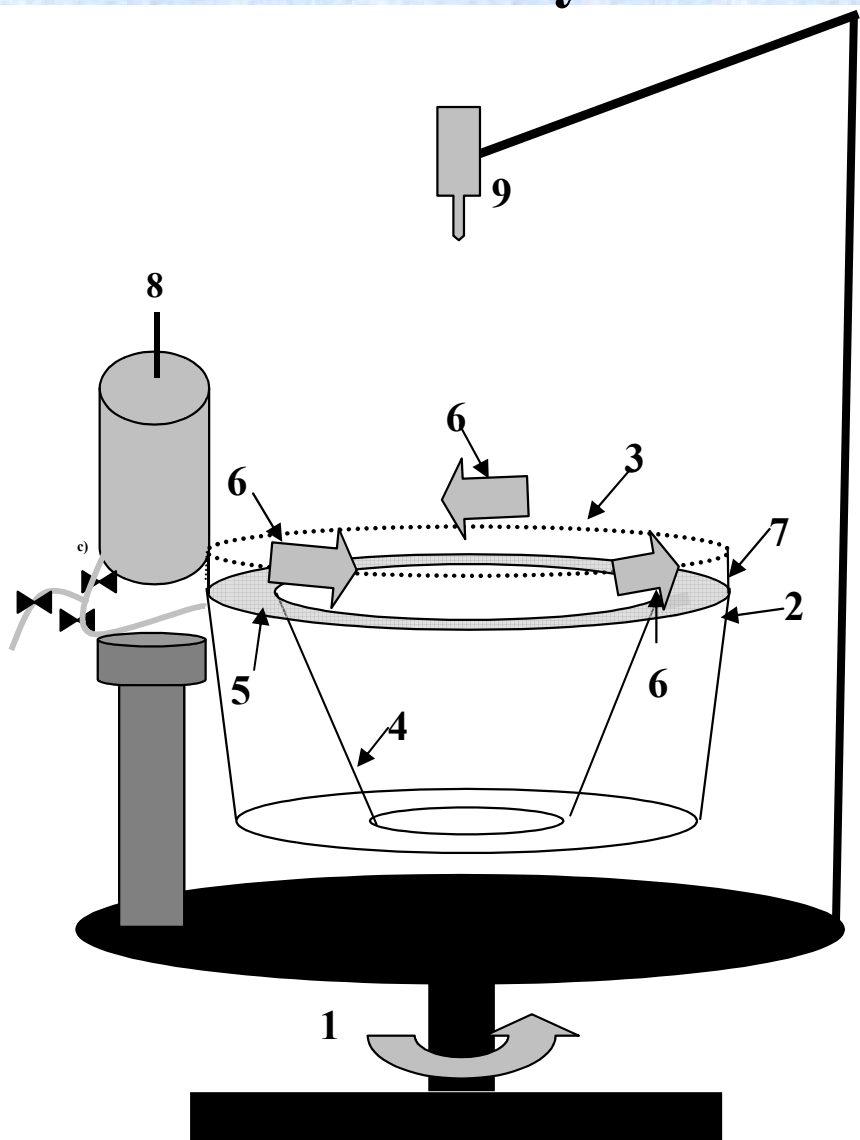
Location of the Rim current core versus the time averaged Ekman pumping velocity ($\langle W_E \rangle$) in the north-eastern Black Sea

In case of strong Ekman pumping ($W_{ek} > 10^{-6}$ m/s) the Rim current core is located over the continental slope.

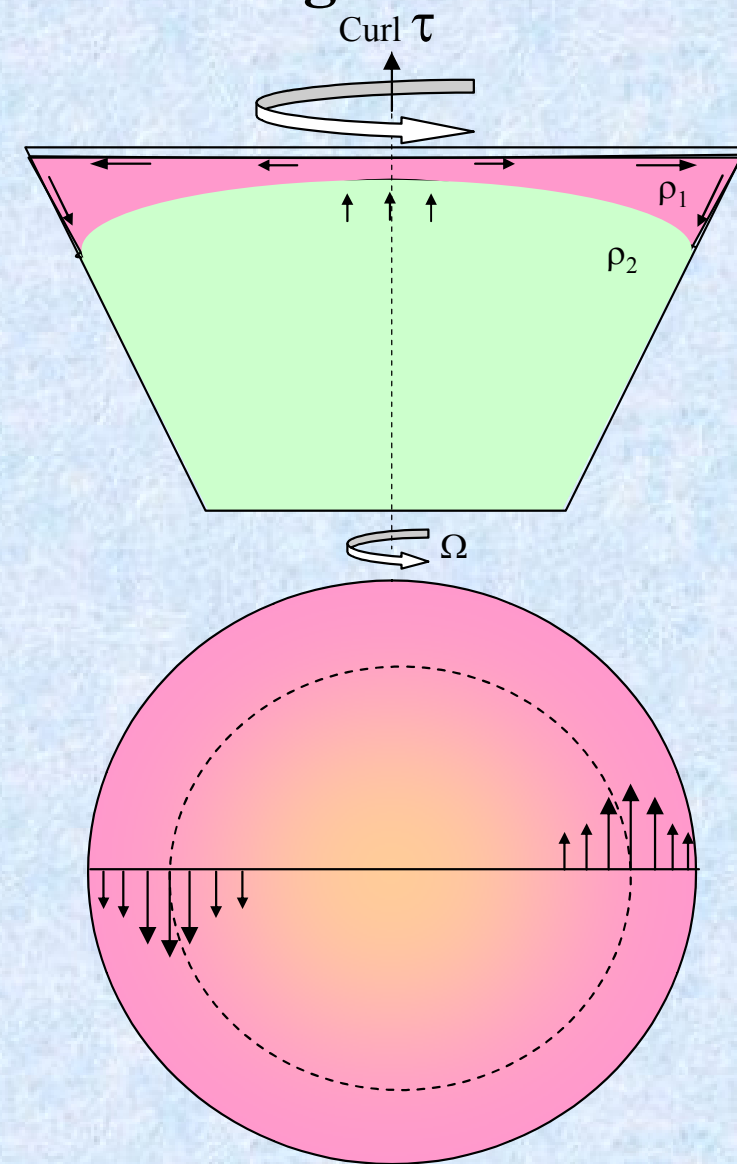
In case of weak Ekman pumping ($W_{ek} < 10^{-6}$ m/s) the Rim current core may be located far from the continental slope.



Laboratory modeling of wind and bottom slope impact on the boundary current in two-layered rotating fluid



1 -rotating platform; 2 –plastic tank with 2-layered fluid; 3 – the tank cap; 4 – sloping bottom; 5 –shelf zone; 6 –wind generators; 7 – wall; 8 – constant flux source; 9 – video camera.

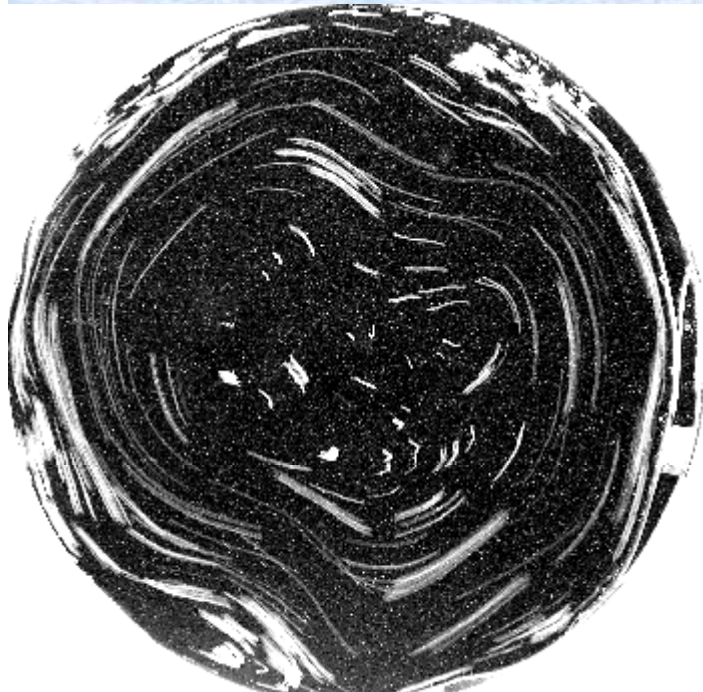


Scheme of baroclinic circulation during the wind forcing phase: side (upper) and top (lower) views

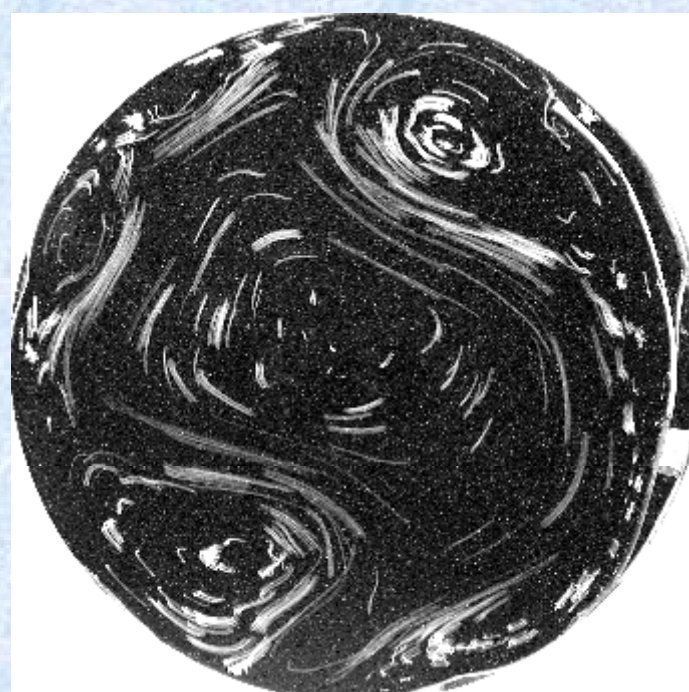
Non-dimensional parameters for the Black Sea and the laboratory model

Parameters (non-dimensional)	Black Sea	Laboratory model
$\theta = h_0/H$	$(0.5-1)*10^{-1}$	$(0.7-1.4)*10^{-1}$
$Bu_0 = (R_d/L_o)^2$	$(0.6-2)*10^{-2}$	$\sim 10^{-2}$
L_S / R_d	0.5-5	1-8
$E = v/(f h_0^2)$	$(0.01-1)*10^{-4}$	$\sim 10^{-3}$
$Fr_{Rim} = U_{Rim}/(g' h_0)^{0.5}$	$(0.4-2.0)*10^{-1}$	$(0.3-3.0)*10^{-1}$

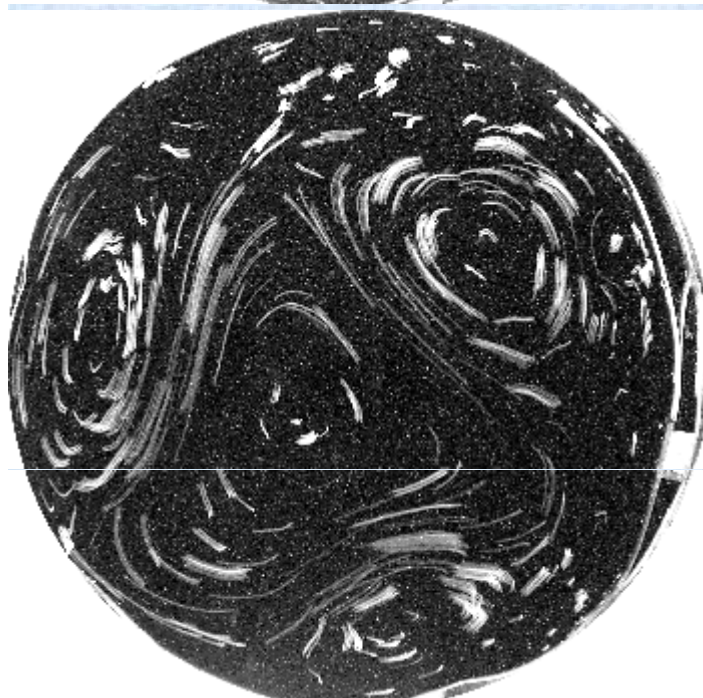
Relaxation of the boundary current formed by Ekman pumping in case of narrow (steep) slope: $L_S/R_d = 1$ (Zatsepин et al., 2005)



Developed boundary current at the end of wind forcing



4 lab. days

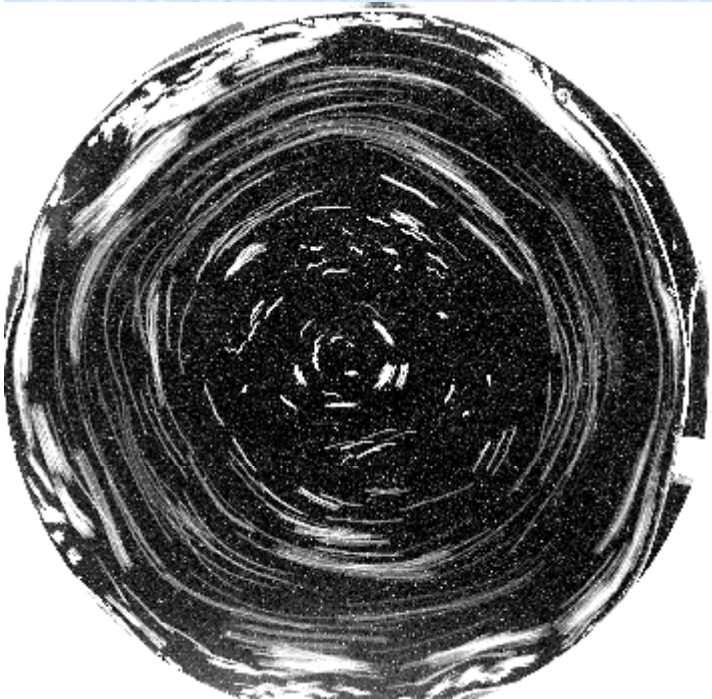


17 lab. days

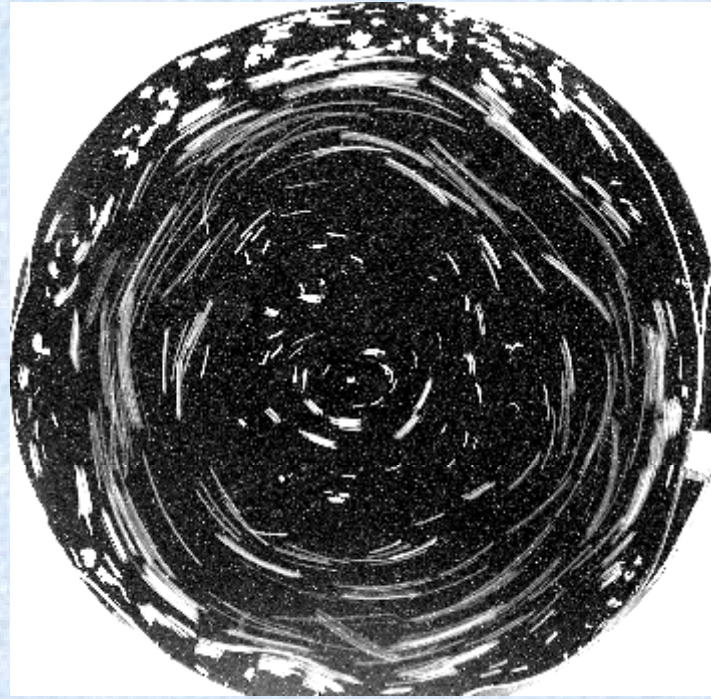


45 lab. days

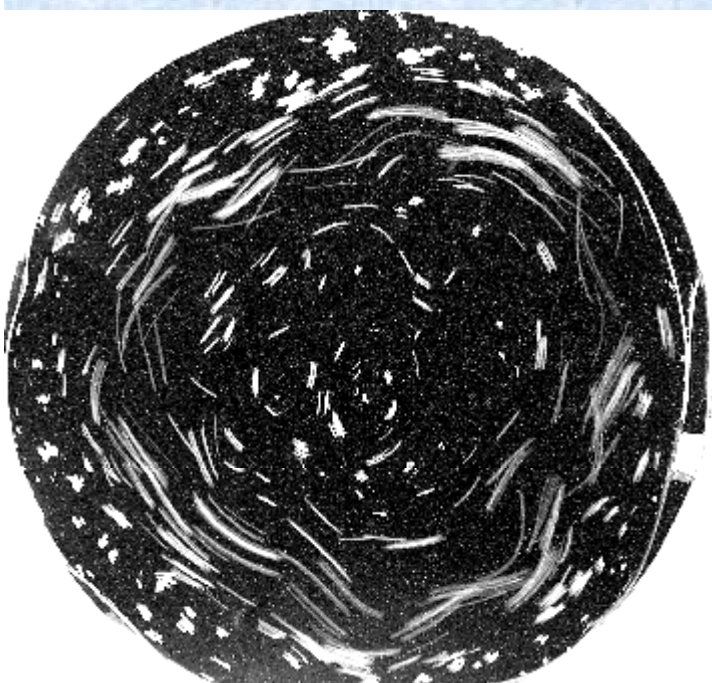
Relaxation of the boundary current formed by wind stress in case of wide (gentle) slope, $L_s/R_d = 4$ (*Zatsepin et al., 2005*)



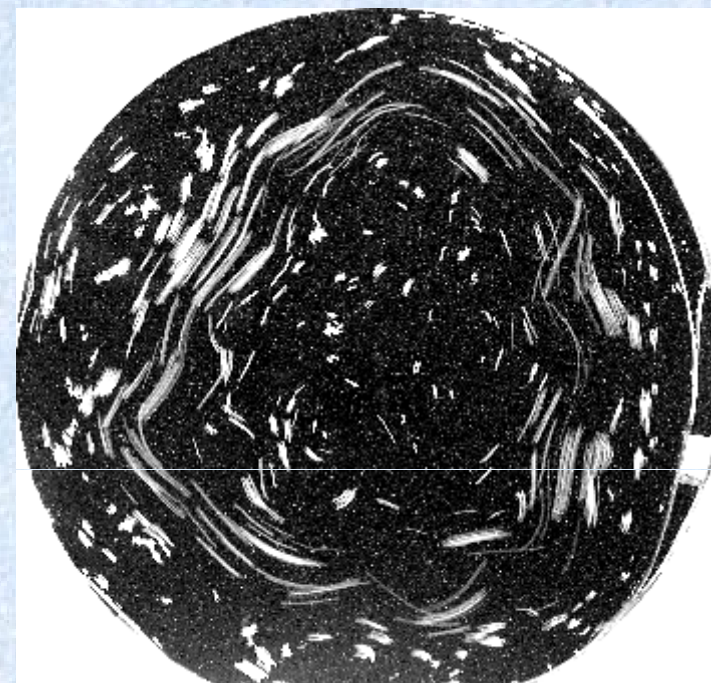
Developed
boundary
current at
the end of
wind
forcing



17 lab. days



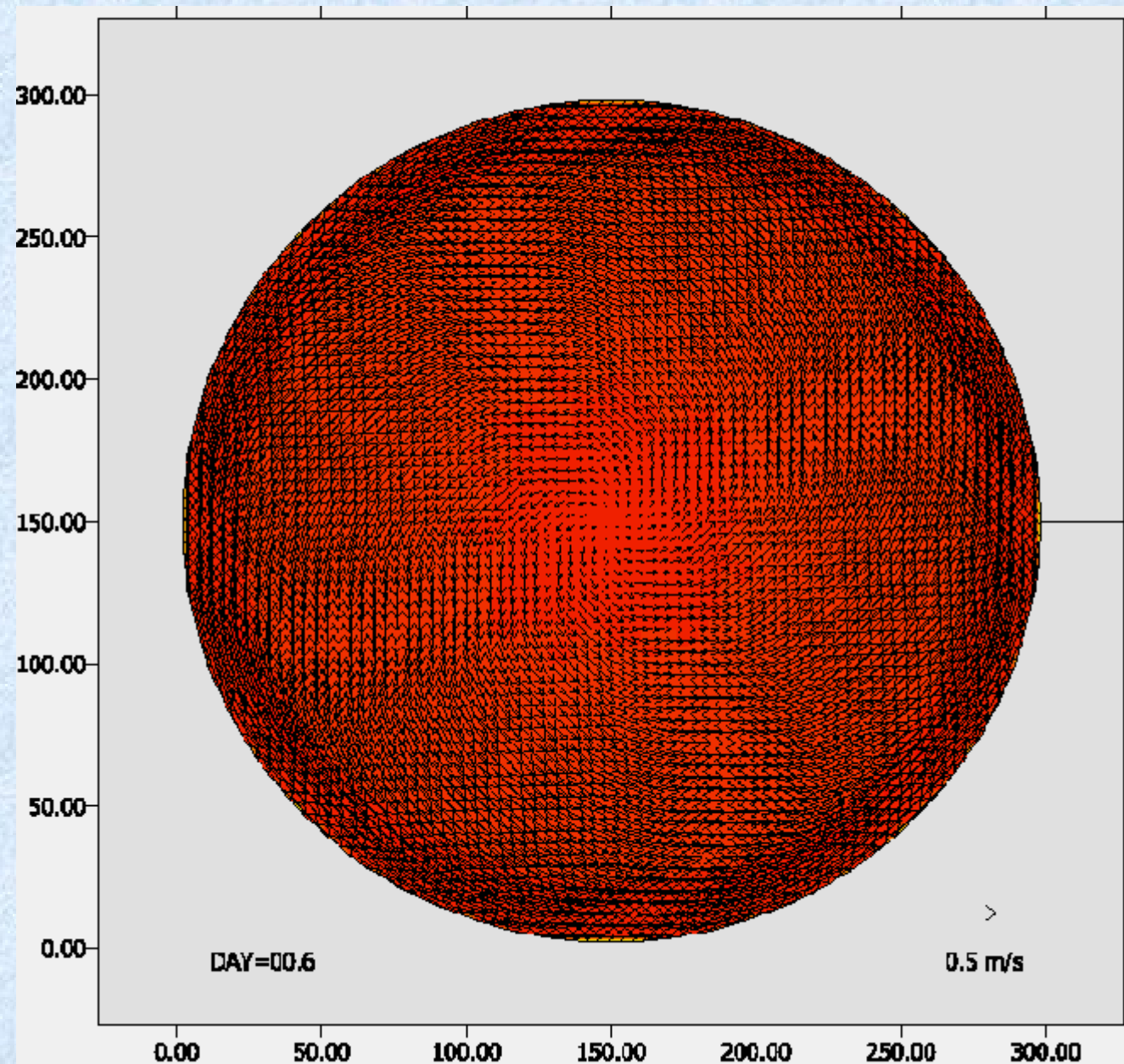
34 lab. days



45 lab. days

Numerical modeling

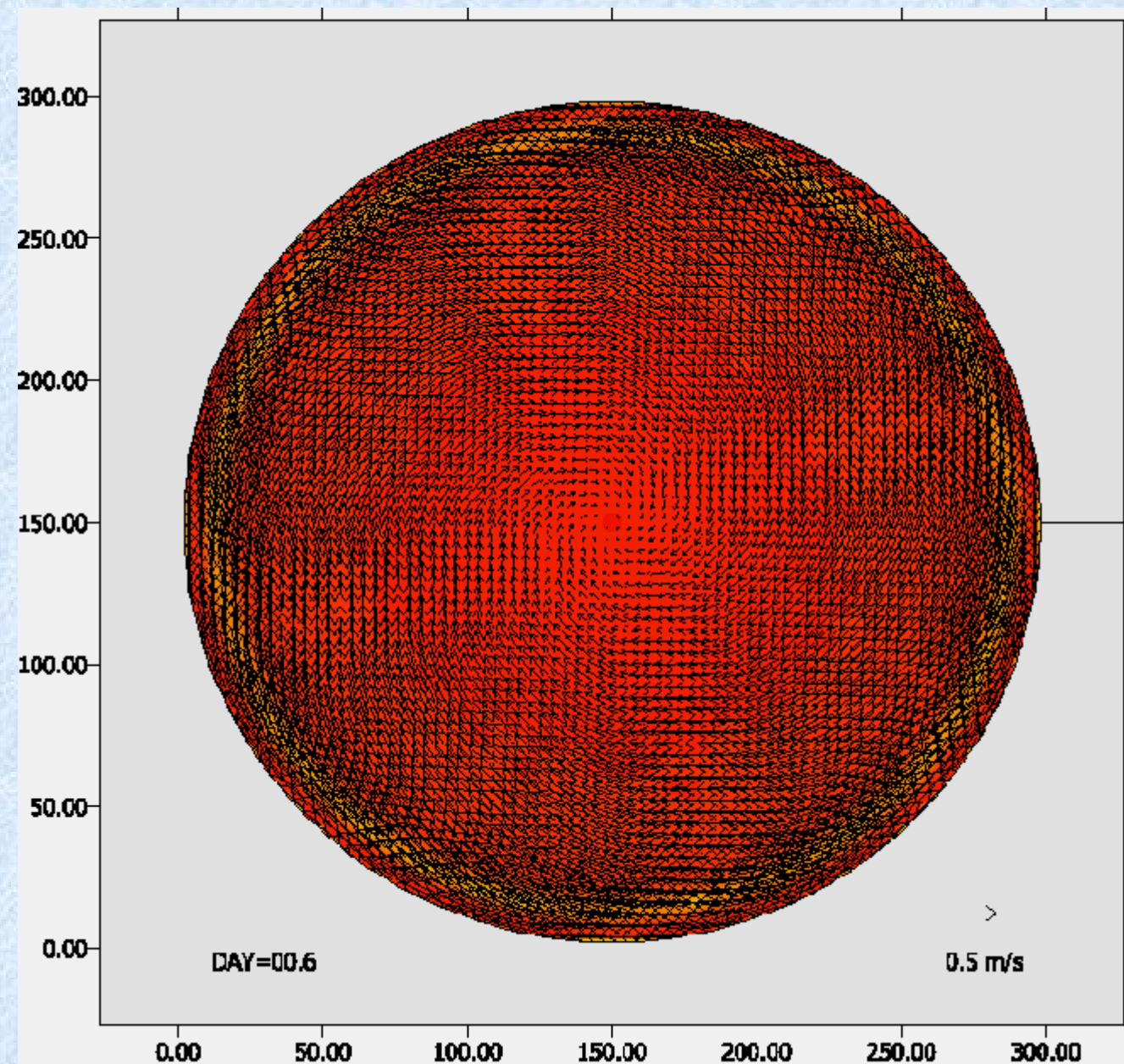
(cyclonic wind vorticity)



Zhurbas et al.,
2005

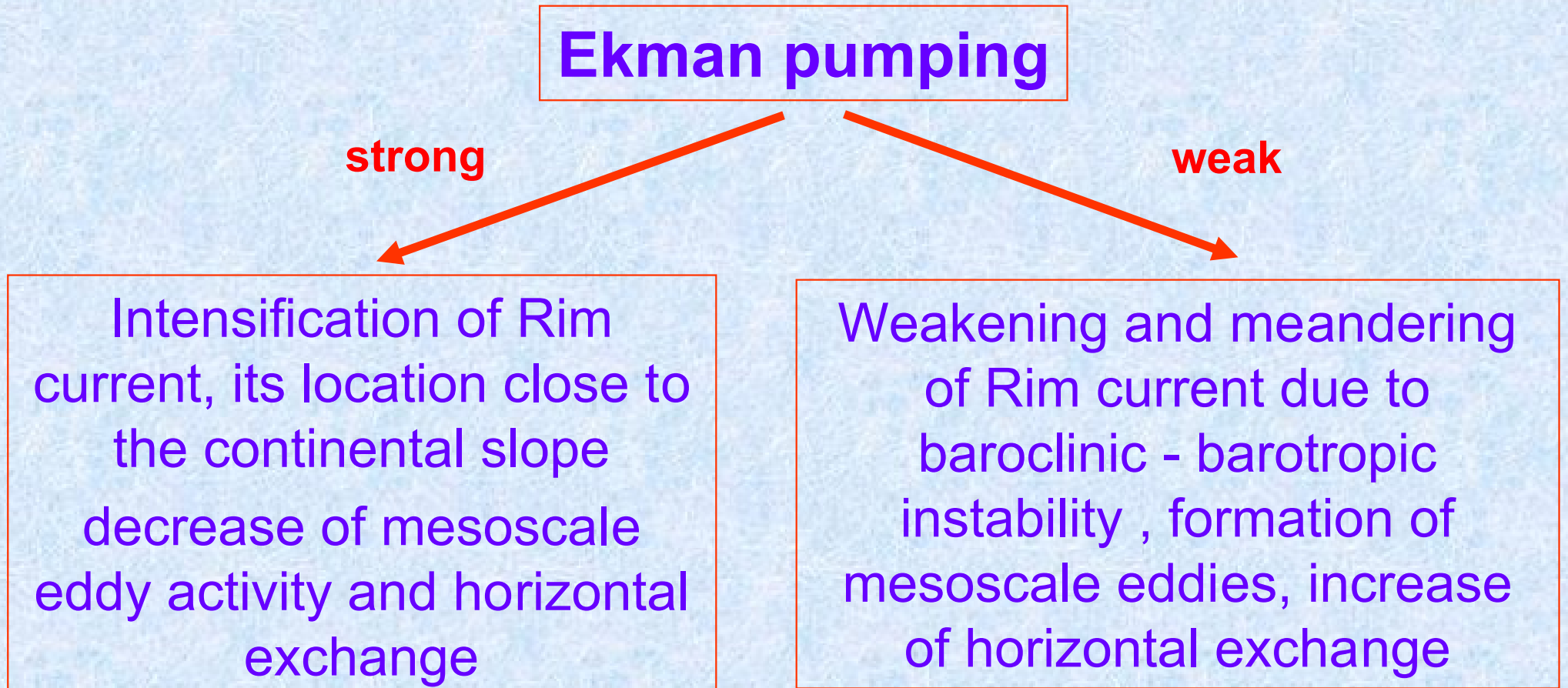
Numerical modeling

(anticyclonic wind vorticity)



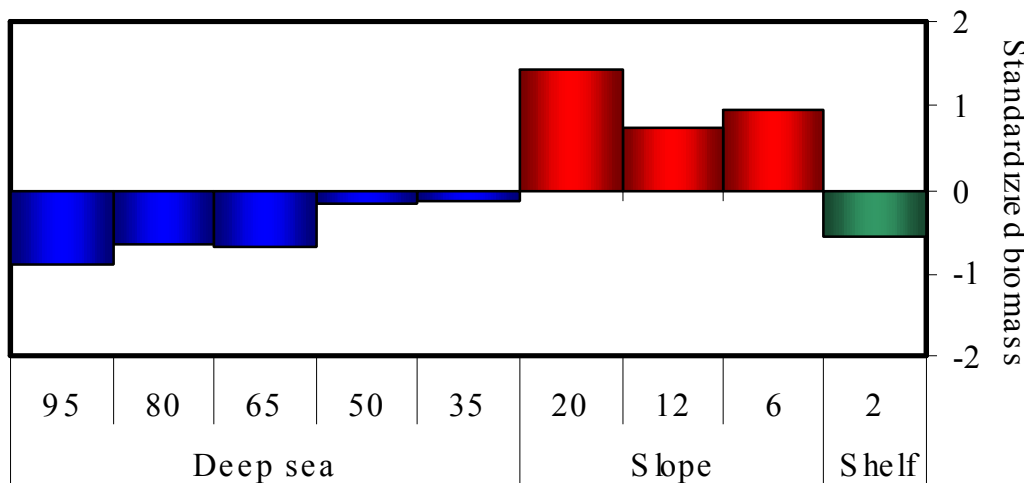
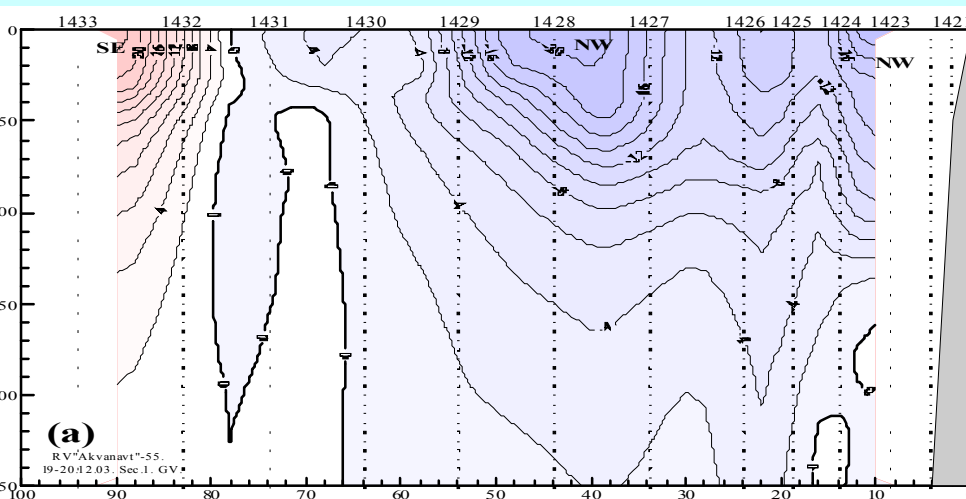
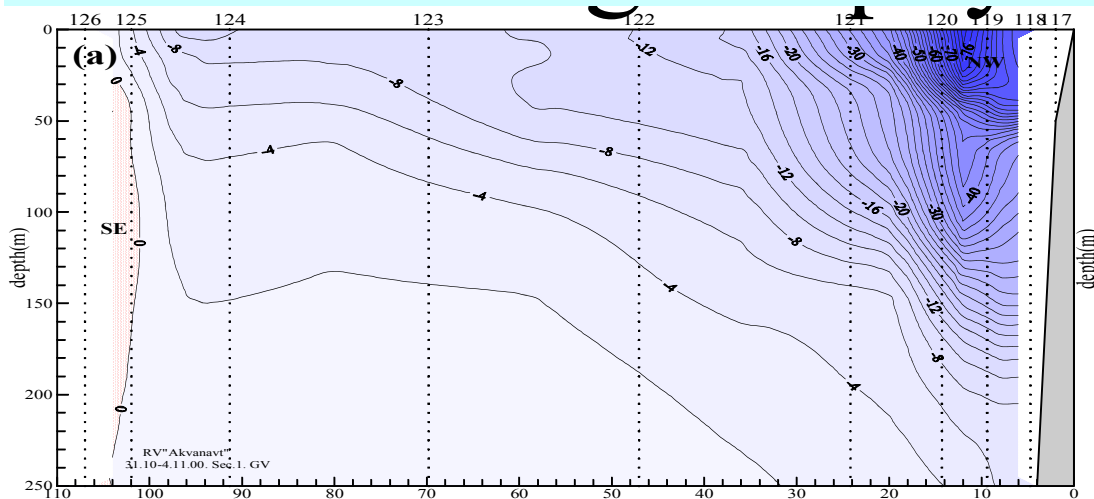
Zhurbas et al.,
2005

Effect of Ekman pumping temporal variability on the Rim current and mesoscale eddy dynamics in case of N.E. Black Sea, cyclonic circulation upon narrow continental slope

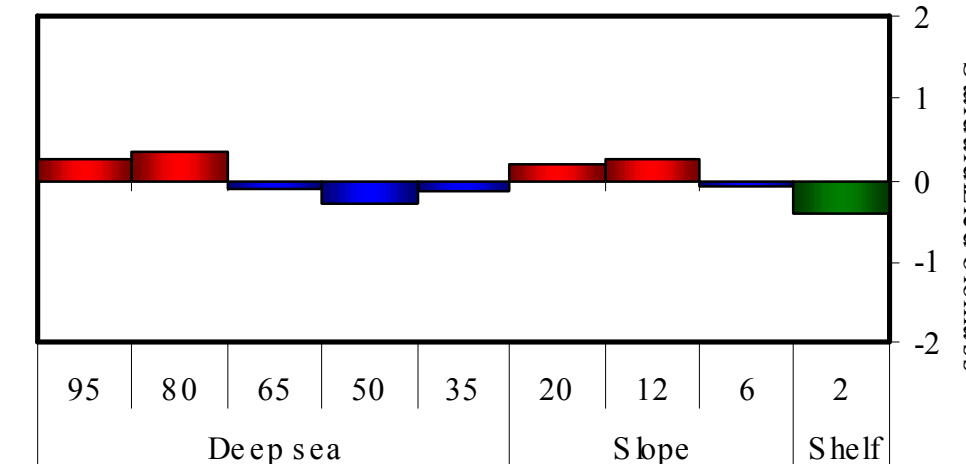
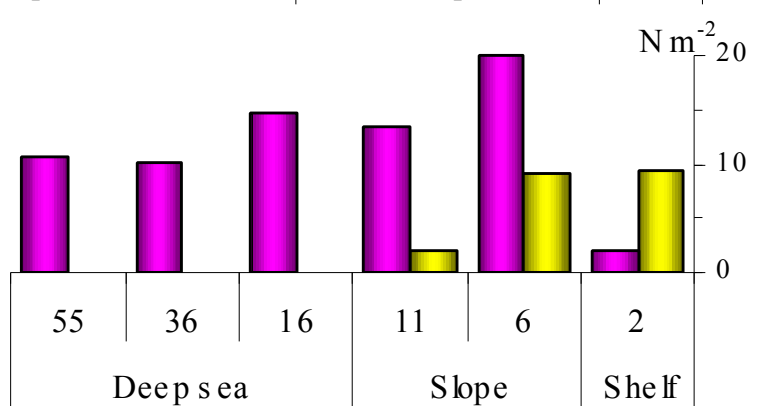


Adjustment time scale to the new Ekman pumping level is about 1 month

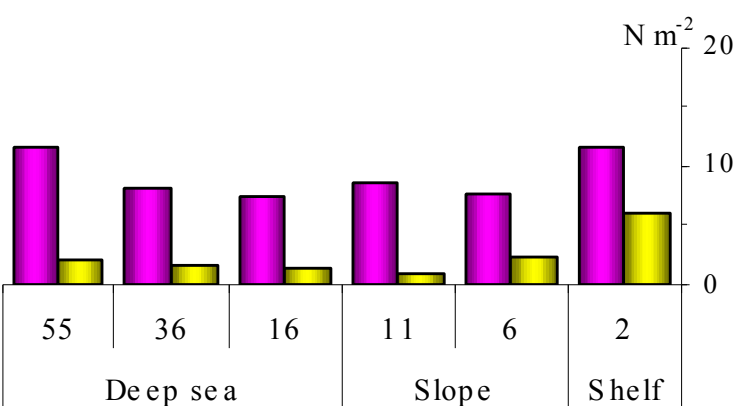
Biological/physical interactions



■ Bivalvia
■ Calanus

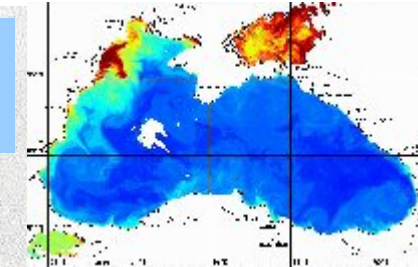


■ Bivalvia
■ Calanus





THANK YOU!



**БЛАГОДАРЮ
ЗА ВНИМАНИЕ**